C.P. No. 1266

C.P. No. 1266

MINISTRY OF DEFENCE (PROCUREMENT EXECUTIVE)

AERONAUTICAL RESEARCH COUNCIL

CURRENT PAPERS

Afterbody Drag Measurement at Transonic Speeds on a Series of Twin and Single Jet Afterbodies Terminating at the Jet-Exit

By

O. M. Pozniak and A. B. Haines,

Aircraft Research Association Ltd.

LONDON: HER MAJESTY'S STATIONERY OFFICE

1973

PRICE 85p NET

CP No. 1266*
February, 1973

AFTERBODY DRAG MEASUREMENT AT TRANSONIC SPEEDS ON A SERIES OF TWIN AND SINGLE JET AFTERBODIES TERMINATING AT THE JET-EXIT

by

O. M. Pozniak and A. B. Haines,

Aircraft Research Association Ltd.

SUMMARY

A systematic series of twin-jet afterbodies all terminating at the jet-exit has been tested at Mach numbers from M = 0.7 to 1.3 on a strut-mounted rig employing high pressure air for the jet streams. The afterbody drag was derived from balance measurements of thrust-minus-drag and wind-off calibrations of thrust, and interpreted with the help of pressure plotting data. Two single-nozzle afterbodies were tested for comparison.

Parameters investigated in the programme include jet size, base area with the changes obtained by infilling the valley between the nozzles and by extending as a fairing, afterbody boattail angle, nozzle shroud area ratio coupled with changes in shroud length, and shroud angle.

At subsonic speeds and likely operational jet pressure ratios, the afterbody drag coefficients based on fuselage cross-sectional area lie in the range 0.03 - 0.06 of which typically, 0.026 can be ascribed to skin friction. Under these conditions, much of the variation between configurations can be expressed as a linear increase in afterbody drag with effective base area suitable defined to represent the area over which the external stream is necessarily separated. In particular, this concept appears to be a means of reconciling the drag of single - and twin - nozzle installations of the present type with the nozzle exits close to the base. The rate of increase is given by 0.12 × effective base area/fuselage cross-sectional area. At M = 1.3, or at higher jet pressure ratios at any Mach number, this simple type of correlation is less successful.

The increase in afterbody drag with shroud area ratio is greater at the higher jet pressure ratios. An increase in shroud angle from 15° to 20° with a boattail angle of 15° increases the afterbody drag coefficient by 0.004 subsonically or 0.007 at M = 1.3; a reduction in boattail angle from 15° to 10° is beneficial at M = 1.3 but gives a small penalty subsonically, due to a poorer pressure recovery at the base.

The tests have produced some "design rules"; the report stresses the factors that should always be borne in mind when applying these rules in practice.

---

*Replaces ARA Report No.29 - A.R.C.34 280

CONTENTS

FIGURES

FIGURES (Continued)

1. INTRODUCTION

For many years, tests on various combat aircraft designs have shown that the afterbody drag of a twin-jet nozzle configuration can be a significant proportion, typically 20% - 30%, of the total aircraft profile drag at zero lift. Being as large as this, it can influence not only the detail design of the boattailed afterbody itself but also the choice of nozzle, the choice of engine bypass ratio and even in some cases, the fundamental decision whether the aircraft should be single - or twin-engined. In cases where the afterbody drag was particularly high at an early stage in the design, it was often possible to obtain improvements during the period of development testing and to understand qualitatively, the reasons for such improvements. Quantitatively, however, the results were a matter for experiment rather than prediction. The only clear design rule emerging from these ad hoc exercises was that the base area should be kept as small as possible but there was constantly the suspicion that for a given base area, the drag of a twin-nozzle installation was greater than for the corresponding single-nozzle layout. By 1967, it had become clear that the results of these ad hoc tests even if fully analysed and correlated would not provide the necessary guidance for the future and that a generalized research programme was needed.

The devising of a useful research programme was far from easy and led to much debate. The flow over an afterbody with twin-nozzle exits can be very complex; it depends on many factors. The geometry itself is strongly 3-dimensional with circumferential variations in the longitudinal curvature distribution; the viscous effects are clearly of paramount importance and finally, the afterbody drag for twin-jet configurations must depend on the interaction of two primary (and possibly, two secondary) streams and the mixing of these streams with the external flow off the base of the afterbody. Theory by itself cannot make an immediate impact on such a situation. Also, it was felt that an experimental investigation in depth into the flow over a single representative afterbody would not be sufficient; rather, what appeared to be needed was an experimental programme in which the afterbody shape was varied in a systematic manner, taking one variable at a time and determining its effect on the afterbody drag. In this way, it was hoped to provide the design "rules" or "numbers" required by aircraft project engineers for exchange rates in early project studies and when choosing the initial shape at the start of the development of a new project. It was accepted that whatever research was undertaken, there would still be a need for development tests on specific designs but the hope was that with the help of the research, these tests could be less time-consuming and more successful in arriving at a true optimum layout.

The above definition of the aim of the research programme may sound sensible but in reality, the problem is not as simple as this The parameters cannot be treated entirely as independent variables. In practice, a change in one variable is likely to be coupled with a change in another variable. Certainly, the effects of a primary variable in any comparison may well depend on the values selected for the other secondary variables. It was therefore realised at the outset that a research programme in which the only measurements were of the overall afterbody drag might be a dangerous undertaking in that without complete understanding of the results, there was the risk that they would be taken out of context and generalized too loosely It was therefore agreed that the overall afterbody drag measurements should be supplemented by some pressure plotting, limited for most afterbodies but extensive in some cases The pressure plotting would at least help to show how the afterbody drag was built up from separate contributions on the boattail, base, secondary duct and shroud external surfaces. Further, the pressure plotting should show how the results depend on the test environment and on the values selected for the variables not immediately under study.

The research programme was planned in late 1967. Apart from the content, scope and nature of the programme, other important issues had to be considered e.g., the choice of test rig, the manner of testing, the nature of the force measurements to be made and finally and most important, whether the chosen rig would give a standard of accuracy commensurate with a systematic study of what might be in the experiment, relatively small differences but in application to an aircraft, very significant differences. Rigs for the provision of accurately defined blowing air whilst attempting to measure either drag or thrust-minus-drag, are inevitably very sophisticated pieces of equipment For the rig that measures the drag directly, the mechanical seal problems associated with small clearances can introduce significant errors. For the rig that on the other hand, measures thrust-minus-drag, one must know the gross thrust of the exit flow to an accuracy compatible with the required accuracy for afterbody drag and a typical figure is that 10% of the afterbody drag, a reasonable and far from extravagant target, corresponds to 1% of gross thrust. At the same time, it is necessary to introduce the blowing air into the model with no interference and to the same order of accuracy. Broadly speaking, there are two different types of rig for such tests With the first, the test afterbody is at the aft end of an axial pipe introduced through the wind tunnel contraction while in the second, the high pressure air is introduced through a support strut usually mounted from the tunnel wall and at right angles to the body under test. The first type of rig has the disadvantage that unless special measures are taken, the boundary layer

on the tube approaching the afterbody is seriously oversized relative to that on the full scale aircraft. With the second type, the main problem is that the pressure field of the support strut can give sizeable interference. For the present research programme, it was decided that the tests should be made on the Rolls Royce 'B.15' rig in the A.R.A. transonic tunnel. This is a strut-mounted gross thrust-minus-drag rig with cold jet flow simulation. This rig has three main advantages:

(i) it had already been used for many of the ad hoc tests and therefore, continuing to use it for the research tests ensured consistency,

(ii) the boundary layer thickness on the afterbody is not seriously unrepresentative,

and (iii) the accuracy and repeatability of measurements on the rig had generally been about 10% of afterbody drag which from the figures quoted earlier, is equivalent to 2 - 3% of total aircraft drag. This accuracy was perhaps marginal but was thought to be about the best that could be achieved on any rig

A further study of the possible accuracy and of the support interference corrections was undertaken as a preliminary to the research programme; these matters are discussed below in sections 3 (and 4.3), and 4.1 respectively.

The choice of rig has some effect on what parameters can be investigated in the research programme. For example, with the B.15 rig, it is difficult to vary the lateral spacing of the nozzles. It was recognized from the outset that the most important single parameter was the longitudinal position of the nozzle relative to the base of the afterbody. It is now common parlance amongst specialists in U.K. to classify twin-nozzle afterbodies as follows:

Class I : aircraft fuselage terminating near the nozzle exits e.g. TSR2, MRCA,

Class II : slender afterbody or spine projecting beyond the nozzle exit plane e.g. Phantom, Jaguar, F-111,

Class III : most of fuselage boattailing occurring aft of the nozzle exit plane e.g. Buccaneer, Harrier

The first phase of the programme concentrated on Class I, with limited variations in this class, tailored to current projects. In total, some 28 configurations were tested, the programme including two sizes of primary jet

and changes in boattail angle, base area, shroud area/jet area ratio and shroud angle. Also, two single nozzle layouts were tested and these provide a link with R.A.E. research on such configurations. Subsequently, in a second phase of testing, the programme has been extended into Class II and now, a third phase covering Class III is being planned.

The force and pressure plotting results from the first phase have been given in detail in refs. 1, 2 respectively. The present report describes what was tested in this first phase and sets out the principal conclusions with sufficient supporting evidence to illustrate these conclusions. The second and third phases will be reported later.

It is worth noting that while the tests have been in progress, test results have appeared from somewhat similar programmes being undertaken elsewhere. Such results are given for example in refs. 3, 4, 5. Hence, a fair amount of systematic data is now being assembled but even so, as noted earlier, there are so many interrelated and interrelating variables that it will still be necessary to test configurations for specific projects for a long time to come.

2. DETAILS OF MODELS AND TESTS

The tests were made on the 'B.15' strut-mounted gross thrust-minus-drag rig in the A.R.A. transonic tunnel. The rig is shown in figs. 1a,b. The forebody and support strut are earthed and a strain gauge balance measures the gross thrust-minus-drag on the metric afterbody aft of a split at a location shown in fig.2. The junction between the external surfaces is in the form of a knife-edge with a small gap of less than 0.008"; internal pressures were measured to obtain a split line force-correction. Unheated compressed air is used to simulate the jets. The rate of flow of the jet air is measured externally in the supply duct and the jet total pressure is measured just ahead of the nozzles by means of special pitot rakes. The overall model dimensions are given in fig.2. The rig and test technique is described in ref.6 and the data reduction in ref.7.

This report is concerned with the tests in the first phase of the research programme in which all the twin-jet afterbodies have their nozzle exits at or close to the afterbody base plane. The definition of the relevant areas is shown in fig.3, 'm' being the fuselage frontal area used for non-dimensionalising the afterbody drags, 'j' the combined area of the two primary jets, 'b' the base area between the nozzle and 's' the combined shroud exit area for the two nozzles. Two primary jet sizes, $j/m = 0.07$ and 0.13 were tested; these represent cold engines of different bypass ratios. The primary jet nozzle was a simple convergent nozzle with an internal contraction angle of 5°. For each of the jet sizes, tests were

made with various shroud area ratios, s/j, in the range from 1.0 to 2.1.

The lower limit of shroud ratio, s/j = 1, with the shroud exit and primary nozzle diameters equal was chosen to be representative of an iris nozzle. The higher limit is representative of a translating shroud associated with a non-reheat primary nozzle whose exit diameter is determined by having to provide adequate clearance of the primary nozzle in the reheat condition in which the primary nozzle area is nearly twice the cold value. Intermediate values imply different degrees of petal shrouding representative of variable ejector nozzles.* When interpreting the results later, one must constantly remember that in these tests, a change in shroud area ratio is always associated with a change in shroud length aft of the base e.g. maximum area/minimum length and vice versa. Practical requirements, e.g. the need to cover the operating mechanism, also determined the shroud angle (θ), and absolute length of the shroud, and thus, the minimum upstream diameter of the shroud duct to which the afterbody boattails had to be faired. For the present tests, the standard shroud angle was $\theta = 15^{\circ}$ but one test was made with $\theta = 20^{\circ}$. There was no flow through the secondary duct for these tests but the models were designed to provide secondary flow should this be required in the future.

Details of the afterbodies tested are shown in Fig.4 and the longitudinal area distributions in Fig.5. The 'datum' configurations were those with b/m = 0.040 and a final boattail angle, β of 15°, Figs.4b,d. The programme** included:

(i) changes in boattail angle, 15° versus 10°, Figs.4b,d,

(ii) changes in base area (j/m = 0.13 only) obtained by infilling the valley between the nozzles to give b/m = 0.0685 and 0.0963, Fig.4c and by extending as an internozzle fairing to give a zero base, Fig.7b,

(iii) comparisons with the single-nozzle configurations in Fig.4a. The 'single' provides the strict comparison with the twin-nozzle afterbodies: the 'short single' provides the link with R.A.E. research on an axisymmetric rig. It should be noted that these two single-jet layouts had their base plane at the same station: for the 'short-single' a parallel section was inserted ahead of the boattailed afterbody (but still on the live part of the model).

The shape of the boattailing was derived mathematically in a consistent manner to fair into the chosen base area and duct size. The final boattail angle was maintained constant around the circumference. This is not a trivial point.

---

*It should be noted that in these tests the primary nozzle and shroud exits are coplanar. However, for shroud exit planes located either upstream or just downstream of the nozzle exit plane, the drag of the nozzle shroud combination is at a minimum and is relatively independent of axial location; this is the range which in reality would most probably be representative of an ejector nozzle in its 'cold' position.

** as listed in Table I.

as will be appreciated from fig.4, the change in body width on the side* was much less than at the other extreme, the change in body height in the valley between the nozzles Hence, the constraint of a constant final boattail angle resulted in greater curvature than would otherwise have been necessary on the side of the boattail at a position close to the base. It is arguable that the choice was an artificial restraint that would not be adopted in practice. It can however be justified on the grounds that otherwise, there would be a discontinuity with a conical shroud.

An important point to note from fig.5 is that the reduction in boattail angle, β , from 15° to 10° being associated with no change in boattail length, implies a significant increase in curvature near the start of the boattail. When generalizing the results, one should consider whether any trends are due to the change in β or the change in shape further forward; the answer to this question could affect the conclusions for some other geometry.

In total, some 28 configurations were tested. The sequence of shroud area ratios was covered for both jet sizes, both boattail angles and for the 'single jet' afterbody; the increased base area cases were tested with s/j = 1.0 and 1.7; the interfairing with s/j = 1.0 only and the 'short single' with s/j = 1.3 only Details of the nozzle and shrouds are shown in fig.6, and a photograph of a typical assembly in fig.7a.

The range of test conditions was:

Mach numbers	Jet Pressure Ratio, PJ/P
0.7, 0.8	1 to 5
0.9, 0.95	1 to 6
1.3	1 to 7

Only the configurations with the larger jet size, j/m = 0.13, were tested at M = 1.3.

A roughness band was located on the cowl nose to promote transition ahead of the test afterbody

For most afterbodies, the external pressure plotting was limited to 26 tappings, distributed 15 on the boattail, 4 on the base, 6 on the external shroud and 1 on the internal shroud with 2 extra pressure tubes inside each of the secondary ducts. Tests with extensive pressure plotting (82 tappings on the boattail and 6 on the base) were made on the twin-jet afterbodies, j/m = 0.13, b/m = 0.0407, $\beta = 10^{\circ}$, 15° with shroud area ratio, s/j = 1.3.

---

* Top or bottom as mounted on the rig. fig 1.

3. REDUCTION AND ACCURACY OF RESULTS

The force data presented in this report are in the form of an afterbody drag coefficient C_{DAI} based on a maximum cross-sectional area, m, defined as shown in fig.3; specifically for these tests, this is the cross-sectional area at the body split at the forward end of the test afterbodies. The values of C_{DAI} have been corrected as described below in section 4.1 for the interference of the forebody and support strut. The afterbody drag is calculated as the difference between the static thrust of the primary nozzle without shroud and the measured wind-on thrust-minus-drag of a given configuration at the same total jet pressure/free stream static pressure ratio, P_J/P, and mass flow function, $W\sqrt{T}$. The drag, as thus defined, includes all effects of the freestream on the external surfaces of the boattail and nozzles and on nozzle efficiency. It seems appropriate to describe these effects as "drag", certainly for this phase of the research programme where the afterbody does not extend downstream of the exits of the convergent nozzles and where therefore, no significant effects of the freestream on discharge coefficient or internal thrust would be expected.

The pressure measurements and the derived pressure drags have not been corrected for support interference but these results are only presented for M = 0.7 and as will be seen later, these corrections are trivial at this Mach number. They become significant at higher transonic speeds; they are then a major issue in the analysis and application of the results, and this is why they are discussed in detail in §4.1.

Attempts were made throughout the programme to improve and maintain the standard of repeatability. Inherently, this is difficult because the afterbody drag is obtained as the difference between two large quantities with a substantial correction for the pressure across the body split junction between the earthed and live parts of the rig. Repeat tests typically showed a scatter of $\pm$0.5lb. This is equivalent to $\pm$0.004 in C_{DAI} at M = 0.9 ~ 0.95 i.e., $\pm$10% of the afterbody drag. For a combat aircraft, a representative figure for the ratio of wing plan area/fuselage frontal area would be about 9 and therefore, expressed as an aircraft drag coefficient, the repeatability would be about $\pm$0.0004 to $\pm$0.0005.

The issue of whether this standard of repeatability is also the standard of relative accuracy of the test data depends on how the data are used in practice. The most common use of the data will obviously be to find the effects of a change in configuration geometry and as in many cases, the jet effects are found to depend on the geometry, these comparisons should be made at representative operating jet pressure ratios rather than jet-off. Indeed, this is the main justification for

tests of this nature. For such comparisons, the accuracy standards are as quoted above for the repeatability although clearly when considering a sequence with more than two points on the curve e.g. for shroud area ratio, the final accuracy of the mean curve should be substantially better. The representative operating jet pressure ratios vary with Mach number and the size of the jet; suitable values are given below:

VALUES OF P_J/P

M	0.7	0.8	0.9	0.95	1.3
j/m = 0.13	2.1	2.5	3	3.4	6
j/m = 0.07	3.2	3.8	4.5	5.1	-

The values for the smaller nozzles, which represent a lower bypass ratio engine, have been taken as 1.5 times those of the larger nozzles so that the comparisons are made at approximately the same nett engine thrust.

Alternatively, the data can be used to obtain a measure of the jet effects. Here, in assessing the accuracy, one must specify what is meant by "jet effects". If one means the difference between "jet-on" and "jet-off", the accuracy for the data presented in this report should again be as quoted above but with the rider that it proved to be very difficult to achieve this accuracy i.e. to ensure consistency between the "jet-on" and "jet-off" results. If, on the other hand, one means by "jet effects", the effects of a boosted jet relative to a free-flow jet with $P_J/P \simeq 2$ at transonic speeds, the accuracy should be very much better, possibly ± 0.002 in C_{DAI}. "Jet effect" corrections to apply to the test results for a normal model of the complete aircraft with free flow through the intake ducts come into the second category. Hence when discussing the accuracy of these corrections, it is less a question of the repeatability than of whether for example, the support interference has been treated correctly - see §4.1 below.

It is worth adding a final comment on the difficulty of obtaining consistent jet-off results. Initially, it was found that the repeatability for these points was only about ± 1 lb. Looking at fig.9 which illustrates the rapid decrease in afterbody drag with small jet flows, i.e. base bleed, it is tempting to suggest that the poorer repeatability, jet off, is due to slight leakage but in fact, this is not believed to be the explanation. Rather, mechanical constraints are thought to be responsible and experience showed that consistency and the normal standards of repeatability could be achieved if the jet-off data were taken

during jet-on runs after some blowing through the rig i.e. the opposite conclusion to what perhaps might have been expected intuitively. All the data presented in this report were obtained in this fashion.

4. GENERAL COMMENTS ON THE RESULTS AND ON THEIR USE IN PRACTICE

4.1. Support Interference Corrections

The primary direct interference of the forebody and support strut was assessed on the basis of measurements of the pressure distributions along the top, bottom and two sides of a cylindrical tube mounted in place of the test afterbodies. As can be seen from the sketch at the top of Fig.8a, the length of the tube was sufficient to ensure that over much more than the region occupied by the afterbodies, the results should be free from any tube end-effects. The pressure distributions plotted in Fig.8a are a mean of those measured along the four lines of tappings; this point is only significant at M = 1.3, even then, only over the forward part ahead of the strut trailing-edge oblique shock. Fig.8a shows that at M = 0.7, the support interference increases the pressures over the forward part of the afterbodies. As the Mach number is increased subsonically, the interference effects grow both in magnitude and downstream extent. Supersonically at M = 1.3, when the strut trailing-edge shock crosses the afterbodies, the pressures are reduced ahead of, and increased behind this shock.

It was assumed that these pressure distributions could be regarded as incremental effects that would be observed whatever afterbody was being tested. On this assumption, corrections to afterbody drag were calculated using the afterbody area distributions from Fig.5. This correction C_{DI}, for the datum twin-nozzle afterbody, j/m = 0.13, b/m = 0.0407, $\beta = 15^{\circ}$ and also, some typical differences between corrections for other afterbodies and for this datum are shown plotted against Mach number in Fig.8b. The corrections are trivial* at M = 0.7 - 0.8 but increase rapidly at transonic speeds before falling to about $C_{DI} = 0.02$ at M = 1.3. The size of these corrections at transonic speeds is a main reason why the afterbodies were not tested at Mach numbers between M = 0.955 and M = 1.3. Even at M = 1.3, the corrections are probably not as reliable as at subsonic speeds; admittedly, they are not as large as near M = 1.0 but this is partly because the increments in pressure over the forward and rear parts of the afterbody tend to compensate for each other. Also, the concept of using a mean pressure distribution to derive the correction is less sound because of the circumferential variation in pressure over the forward part of the afterbody; fortunately, the slope of the boattail is relatively small over the area affected and so, one can still hope that

---

*The corrections, as computed using the mean pressure distribution and afterbody area distribution, lie in a band $-0.001 < C_{DI} < 0.003$; but by any method of allowing for the variation in the interference pressure field around the afterbody under test

$C_{DI} < \pm 0.004$

the corrections are not seriously in error.

Figure 8c gives two examples of how these support interference corrections can affect the results. First, before applying the corrections, C_{DA} for the datum and indeed, for most other configurations decreases with Mach number between M = 0.8 and 0.955 but this is completely misleading; having applied the correction, C_{DAI} increases with Mach number in this range. The second graph shows that in an extreme case, the corrections can even affect a comparison between two afterbodies: the "short single" has a higher drag tnan the standard length "single" but the effect of the corrections is to notably reduce the difference at transonic speeds and to increase it at M = 1.3. The last comparison can be interpreted by saying that with the "short single" with its parallel section ahead of the boattail, the drag is less affected by the pressure field of the support strut and as can be deduced from fig.8a, this implies a smaller correction subsonically but a larger correction at M = 1.3.

It is important to understand the nature of the interference corrections as derived above and to realise that in principle there may be other interference effects not covered by these corrections. In inviscid, subcritical flow, the corrections as derived represent a buoyancy effect for which there should be an equal and opposite effect induced by the metric afterbody on the earthed support strut and forebody. If one had used an external balance to measure the drag of the full model and support strut, the corrections - again on the assumption of inviscid, subcritical flow - would not exist; similarly, for the complete, full-scale aircraft, the corrections would not exist. In these tests this buoyancy effect is part of the force measured by the balance and so it must be removed before the results are used for aircraft design. To the extent that the corrections are caused by the effects of the viscous wake or the trailing-edge shock of the support strut, there is not necessarily any compensating effect but it was still thought appropriate to apply the corrections in full. It would not have been easy to separate the buoyancy contribution from the remainder; also, it would have been coincidental if the effects of the support strut had been exactly the same as those of say, the wings of the real aircraft.

A more serious issue is whether it is correct to treat the pressure field of the forebody and strut as a simple incremental effect or whether the existence of the pressure field will modify the boundary layer or supercritical flow development on the boattailed afterbody and thus, give what will be termed below as a "secondary" effect or correction. A detailed analysis of the measured pressure distributions suggest that for the present tests at least, these secondary effects should be small at Mach numbers up to M = 0.95 and also probably, not too

serious at M = 1.3. This would not be true for Mach numbers between M = 0.95 and M = 1.3 and so this is another reason why no tests were made in this range.

In support of the claim that these secondary interference effects can be ignored in correcting the data as presented in this report, one can list the following points:

(i) Figure 8a shows that at M = 0.70, 0.90 and 0.955, the sizeable effects of the support interference pressure field are largely confined to the forward third of the test afterbody whereas as shown later in fig.10, the jet effects are largely confined to the rear half of the afterbody. There is thus no direct interplay between the support interference and jet effects,

(ii) Also from figs. 8a, 10, it can be seen that the interference pressure field does not extend far enough downstream at M = 0.7 to affect the peak suction values at the start of the boattail. This is still true up to M = 0.955 and without this influence, it is difficult to conceive that the pressure field has any major effect on the supercritical flow development or on the boundary layer growth in the adverse pressure gradient downstream of this peak suction,

(iii) An increase in Mach number from 0.7 to 0.955 has little effect on the pressures measured on the rear half of most afterbodies while the changes on the forward part of the boattail are very similar to those measured on the cylindrical tube. This would have been a most unlikely coincidence if there had really been any serious secondary effects,

(iv) At M = 1.3, the pressure distributions suggest that the secondary interference should still be trivial on the top and bottom of the afterbodies (as mounted on the rig, fig.1) but could be more substantial on the sides i.e. downstream of the strut. On the top and bottom, the pressure-rise through the interference field (smaller than for the mean distribution plotted in fig.8a) is perhaps only 10% of the pressure-rise through the shock near the base of the afterbody; also, downstream of the first pressure-rise there is an extensive region of largely uniform pressure. On the sides, however, the pressure-rise in the interference field is greater than that shown in fig.8a and although it is still well ahead of the peak suction on the boattail, it could then be argued that the thickening of the boundary layer through the first pressure-rise could affect what happens further downstream e.g., it could ease the effective curvature distribution and reduce the peak suction or on the other hand, it could make the

boundary layer more prone to separate in the final adverse gradient. Hence, one would hesitate to say that the secondary corrections are as trivial as at subsonic speeds up to M = 0.95.

It is fortunate that one can dismiss the secondary effects to the extent described above because it would not have been easy to predict them quantitatively. This is not however the end of the story. The user of the data must still ask himself whether significant secondary effects could exist on his full-scale aircraft design. The most obvious example where there could be appreciable adverse effects is when a fin or tailplane is mounted on the afterbody in a position such that the peak suction induced by the fin or tailplane is roughly at the same fore-and-aft station as the natural peak suction at the start of the boattail. Alternatively, careful positioning of the surfaces such that the peak suction on the boattail was reduced by being immediately downstream of the trailing edge of either the tailplane or the wing of the aircraft could lead to sizeable favourable interference. This may appear to be merely a restatement of the case for applying area rule to a combat aircraft configuration to improve performance at transonic speeds but it is nevertheless, an important point in the present context because this possibility of adverse/favourable interference could in principle at least, undermine the validity of the "design numbers" appearing out of these test afterbody comparisons. Perhaps more particularly, with the aid of favourable interference, one might have been able to consider afterbodies whose local geometry was outside the range of those thought suitable for test in the present programme. To quote just one illustration, the programme includes a comparison between boattail angles of 15° and 10°; the results show that at subsonic speeds, 15° is slightly preferable. Despite this conclusion there was no move to test an angle of say 20° because it is generally assumed that an increase to 20° would be inadmissable because of the boundary layer separation at the rear of the boattail. However, if by favourable interference, one could reduce the peak suction at the start of the pressure-rise on the boattail, one might find that 20° was acceptable. The remarks about support interference have therefore assumed a wider significance. The fact that support interference has had to be looked at carefully at transonic speeds carries the lesson that a study of how the wing, fin and tailplane of the real aircraft affect the flow over the boattail ahead of the twin-jet exits could be another profitable area for research. Pressure plotting would be essential in this case.

To summarise therefore,

1. At M = 0.7, the support interference is trivial and hence for this Mach number, it is fair to present the pressure data uncorrected for support interference

2. At higher Mach numbers, the interference is more substantial. To a great extent, the interference is a buoyancy term with no parallel on the complete aircraft. Corrections based on the pressures measured on the cylindrical tube should therefore be applied. Only corrected force data are presented in this report,

3. No corrections have been applied for secondary effects such as the influence of the pressure field of the forebody and strut on the supercritical-flow and boundary-layer development on the particular afterbody under test. Such effects are likely to be small at Mach numbers up to M = 0.95 and not too serious even at M = 1.3. Similar effects due to the wing, fin or tailplane of the real aircraft could however be significant and could be either favourable or adverse according to the design of the aircraft.

4.2. Afterbody Drag: Breakdown into Skin Friction and Pressure Drag

The values of C_{DAI} presented in this report are based on the total afterbody drag. To assess whether the values are high or low, one must estimate how much of the drag can be ascribed to skin friction. This has been done in various alternative ways viz:

(a) using flat plate theory and a boundary layer thickness measured at the start of the live section with a similar forebody during another series of tests,

(b) using the flat plate theory and with a boundary layer assumed to start at the nose of the forebody,

(c) using a mean value of boundary layer thickness from (a) and (b) and flat plate theory to obtain a boundary layer shape parameter at the start of the live section and then calculating the skin friction on an equivalent axisymmetric body with a pressure distribution equal to the mean measured boattail pressure distribution,

(d) by integrating the measured pressure results to give a pressure drag and subtracting this from the measured total afterbody drag.

Fortunately, these four methods gave results that were reasonably consistent. For the datum twin-jet afterbody with j/m = 0.13, b/m = 0.0407, $\beta = 15^{\circ}$, s/j = 1.3 at M = 0.8, the values of C_{DF} obtained by the four methods were respectively 0.028, 0.026, 0.024 and 0.029. Also, the difference between the total and pressure drags at M = 0.7 - 0.8 was much the same for all the

afterbodies tested. This is what one would expect: the surface areas of the twin-jet afterbodies differ by no more than 2% and even the "short single" has a surface area of only 4% less than the datum twin-jet referred to above.

It is convenient here to refer to fig.21 which presents on a single figure, the values of C_{DAI} for all the test afterbodies at their representative jet operating pressure ratios. It will be seen that the values of C_{DAI} range from about 0.03 to 0.06 of which from the above, one can say that typically, 0.026 can be ascribed to skin friction. This shows that the excess drag is small at low effective base areas (see section 5.5 and fig.20 for a definition of "effective base area").

The general consistency in the trends for the total afterbody drag and for the integrated pressure drag is illustrated in figs. 12a,b. From such comparisons one can conclude that:

(i) the pressure results are substantially reliable in indicating the drag breakdown into components from the boattail, base, shroud surfaces etc.,

(ii) the integrated pressure drags indicate the jet effects with good accuracy, and by inference, the effects on the same boattails due to different nozzle shroud combinations and fairing are correct,

and (iii) finally, in view of the consistency between the results for the two boattail angles, for comparisons where the changes in body geometry are only mild, the relative drag breakdown is again obtained with reasonable accuracy.

These conclusions are implicit in much of the text of the rest of this report.

4.3. Jet Effects

The variation of C_{DAI} with jet pressure ratio is shown in fig.9 for three configurations. These results are typical of those obtained throughout the test series and also, they are consistent with the familiar pattern obtained in other investigations[8,9]. At very low jet pressure ratios, there is a rapid reduction in C_{DAI} relative to the jet-off value but then, C_{DAI} increases to a maximum generally occurring near $P_J/P = 3.0$ before decreasing again at higher jet pressure ratios. This behaviour is attributed in refs. 8, 9 to the interplay of jet pluming and entrainment effects.

Qualitatively, therefore, the behaviour is similar for all the test configurations but quantitatively, the effects both in the initial base-bleed part of the curve and at higher jet pressure ratios vary with configuration and with Mach number. In particular, the jet effects become markedly less favourable as

the shroud area ratio is increased (and shroud length decreased). fig 9 but they also depend significantly on other parameters such as boattail angle To study this, let us consider what happens on the component surfaces

First, fig.10 shows how the jet effects at subsonic speeds e.g. M = 0.7 propagate up the boattail The jet effects reduce progressively in magnitude with distance upstream of the base and when these distributions are plotted against Z rather than X, it is found that in terms of drag, the effects over the forward third of the boattail are negligible In passing, it may be noted that there is a suction peak near X/L = 0 92 particularly on station 1 but to a lesser extent on stations 2 and 3 also This is caused by a sudden change in the slope of the afterbody and is partly due to having specified that the final boattail angle should be constant around the periphery. If this requirement had been relaxed, this peak suction would have been less pronounced but in the context of the present discussion of jet effects, the important point is that both this peak suction and the other more general peak suction occurring further forward at about X/L = 0.7 are reduced by the jet effects. It follows that the appearance of local supersonic regions are postponed to higher Mach numbers as the jet pressure ratio is increased. This is the explanation why the jet effects on C_{DAI} vary with Mach number between M = 0.7 and M = 0.95. For example, taking two of the configurations from fig 9, we find:

For	$s/_j$	ΔC_{DAI} from M = 0.7 to M = 0 95		
		Jet-off	$P_J/P=2$	$P_J/P=4$
j/m = 0.13, b/m = 0.0407, $\beta = 15^o$	1.0	0.013	0.006	0.003
	2.1	0.017	-0.002	0

As forecast above, the variation of jet effects with Mach number can be better described by saying that the increase in C_{DAI} with Mach number up to M = 0.95 that is found jet-off is alleviated by the jet and by increases in P_J/P At M = 1.3, results (not presented here) show that the jet effect at least up to the maximum pressure ratio of the tests is confined to the trailing edge of the body aft of the start of the shroud for station 1 (fig.10) and slightly further forward at the valley station 4.

Figure 13 shows how the jet effects at M = 0.7 on the integrated pressure drag on the boattail vary with the test configuration. It will be seen that the jet effects are at their most favourable for the single-nozzle afterbody faired to a

zero base and are less pronounced for the twin-nozzle configurations with a finite base between the nozzles. They deteriorate further with increases in shroud area ratio and base area and also vary in detail with boattail angle. Similarly, figs. 14a,b show how the jet effects on base pressure and secondary duct pressure at M = 0.7 vary with the test configuration. In general, the secondary duct pressure is decreased (and thus, the contribution to C_{DA} increased) by an increase in shroud area ratio and a decrease in boattail angle from 15^{o} to 10^{o}. Increasing P_J/P tends to strengthen the adverse effect of s/j (e.g. the value of P_J/P up to which there is a fall in secondary pressure increases with s/j) but weakens the adverse effect of the reduction in β . The changes in base pressure are a somewhat complicated amalgam of what has been observed for the boattail and secondary pressures.

To summarise therefore, it has been shown that :

(i) the jet effects (but not the jet-off data) depend on the nozzle geometry. Hence, in particular, the corrections needed to convert data from a normal complete aircraft model test with unpressurised jets to boosted jet conditions at an operational jet pressure ratio must be determined from tests in which the details of the nozzle geometry are fully represented,

(ii) the jet effects depend on the afterbody geometry: generally, increasing P_J/P tends to alleviate effects of geometry observed in jet-off conditions. Jet effects from simple nozzle tests without the preceding afterbody represented could therefore be misleading.

The only relieving feature is that even at subsonic speeds, the jet effects do not penetrate to the forward end of a typical afterbody while at supersonic speeds they are confined to the region near and aft of the base.

5. EFFECTS OF CHANGES IN CONFIGURATION

Sections 3 and 4 above have commented on how the data should be interpreted and used in practice. This section 5 considers the effects of the main geometrical parameters. Sufficient data are presented in figs. 9 - 21 to illustrate the most important trends; a reader interested in the full results for a specific configuration should consult refs. 1, 2 if they are not included here.

5.1. Effect of Shroud Area Ratio, s/j

The full range of shroud to jet ratios s/j = 1.0, 1.3, 1.7 and 2.1 was tested with five different boattails. Four of the boattails were twin-jets with a base area ratio of b/m = 0.0407 comprising two primary jet sizes each in combination with two boattail angles $\beta = 10^{\circ}$ and 15°. The fifth boattail was a single jet with j/m = 0.13 and $\beta = 15^{\circ}$. In addition, two twin-jet boattails of j/m = 0.13 and $\beta = 15^{\circ}$ with base area increased by infilling of the valley between the nozzles giving b/m = 0.0685 and 0.0963 were each tested with two shroud ratios of s/j = 1.0 and 1.7. These comparisons involved a total of 24 configurations.

The variation of C_{DAI} with shroud area ratio at the typical operational jet pressure ratios quoted earlier is shown in figs. 11a,b. In general, the afterbody drag increases with shroud area ratio. As would be expected the increase is greater for the larger jet size, j/m = 0.13. The increase is not significantly dependent on Mach number at subsonic speeds and is similar for both the single and the twin nozzles and up to a point, for both boattail angles. There is however some apparent tendency for the rate of drag increase to be more rapid at higher s/j for $\beta = 15^{\circ}$ but not for $\beta = 10^{\circ}$. It may be doubted however whether the accuracy of the data as quoted earlier is sufficient to accept this as a definite genuine conclusion.

The effect of shroud area ratio on the components of the pressure drag at M = 0.7 and the selected operational jet pressure ratios is shown in figs.12a,b. It will be seen that at these relatively low pressure ratios, the effect of varying shroud area ratio on the combined boattail and base drag is small, being largest on the single-jet configuration. One must therefore ascribe the large increase in total afterbody drag to the increase in the contributions from the external shroud surface and the secondary duct. Figures 12a,b indeed show that the sum of these contributions gives a rate of increase with s/j that is very similar to that observed in the overall balance results.

At higher jet pressure ratios, the increase in C_{DA} with s/j tends to be greater, fig.9 and also, there is more dependence on other parameters. This is shown for example in fig.13 for the contribution to C_{DA} from the boattail. It appears that as regards this contribution, the largest effect of shroud area ratio is found on the single-jet body where at the highest pressure ratio of the tests, the largest shroud gives an increment in boattail drag coefficient of about 0.005 as compared with about 0.002 for the datum twin-jet afterbody at its operational jet pressure ratio. The effect of shroud area ratio is least for the boattail with the largest base area and presumably the base of the twin-jet afterbodies tends to act as a buffer.

Figures 14a,b show the effects of shroud area ratio on secondary duct pressure and base pressure. The effects on secondary pressure have already been discussed in Section 4.3 but some comment on the base pressure results is perhaps worthwhile. With the smaller jet nozzle, j/m = 0.07, the base pressure always decreases with an increase in shroud area For the large jet nozzles, j/m = 0.13, however, the results are more confusing. With $\beta = 15^{\circ}$, below a jet pressure ratio of about 2.5, the variation with shroud area ratio is in the opposite sense. This is an example of where one should remember that an increase in shroud area ratio is always accompanied by a movement forward of the jet nozzles towards the base. One can surmise therefore that the initial decrease in C_{DA} with P_J/P is greater for the large shroud area ratios because the jet exits are close to the base and therefore the base is more sensitive to the jet effects whereas at higher jet pressure ratios, the high secondary pressures and their more rapid increase with jet pressure ratio at small shroud area ratios becomes the dominant factor in controlling the base pressure.

5.2. Effects of Boattail Angle and Shroud Angle

Twin-jet afterbodies with terminal boattail angles of 10° and 15° were tested with shroud area ratios of s/j = 1.0, 1.3, 1.7 and 2 1 and primary jet ratios of j/m = 0.07 and 0.13.

The afterbody drag for both boattail angles is shown in fig.11a. The comparison is for the typical operational jet pressure ratios quoted earlier. Taking the results for $\beta = 15^{\circ}$ as the datum, the change to $\beta = 10^{\circ}$ reduces C_{DA} at M = 1.3 by about 0 006 - 0.008 but gives a slight increase in C_{DA} at subsonic speeds by perhaps 0.002 - 0 004. To judge from the component drags obtained from the pressure results at M = 0.7 in fig.12, the change to $\beta = 10^{\circ}$ is successful in reducing the actual boattail drag at subsonic speeds but this improvement is more than offset by an increase in the contributions from the base and shroud surfaces. To quote one set of figures as an example:

ΔC_{DA} FOR CHANGE IN β FROM 15° TO 10°

M = 0.7, j/m = 0.13, s/j = 1.3

Boattail:	-0.004
Base :	0 002
Shroud surfaces:	0.004
Total :	0.002

The dependence of the final result on shroud area ratio is not great but the results suggest that if there had been less rearward-facing surface to be influenced by the pressure recovery at the base, the change to $\beta = 10^{\circ}$ might have been favourable even at subsonic speeds.

Clearly, the choice of β for an aircraft project will depend on the operational requirement e.g. on the relative emphasis on subsonic and supersonic flight conditions but also, the choice depends on the interpretation placed on the present data. There is a difficulty at this point. It is clear that the slightly poorer results at subsonic speeds with $\beta = 10^{\circ}$ is because there is less pressure recovery at the base but this result can be explained in two different ways. The poorer pressure recovery may either be due to the discontinuity in contour between the 10° boattail and the 15° shrouds used in the present tests or alternatively, it may be inherently due to the fact that the lower boattail angle requires less turning of the external flow in the vicinity of the base. It may of course be due to a combination of these two factors. On the first explanation, the implication is that if the shroud angle had also been changed from 15° to 10°, the results at subsonic speeds for $\beta = 10^{\circ}$ would have been improved. On the other hand, if the second explanation is correct, this leads to the conclusion that for optimum performance at subsonic speeds, one should increase β to the maximum value that can be used without provoking a boundary layer separation on the rear of the boattail.

It is tempting to link these results with those obtained when with $\beta = 15^{\circ}$, the shroud angle was increased to 20°. Figure 9 shows that this change in shroud angle gave a notable increase in C_{DA}, varying somewhat with jet pressure ratio but typically, about 0.004 at subsonic speeds or 0.007 at M = 1.3. Admittedly, the combination $15^{\circ}/20^{\circ}$ gives a discontinuity in slope at the boattail/shroud junction similar to that obtained with $10^{\circ}/15^{\circ}$ but the change in shroud angle to 20° does more than this: it reduces the length of the shrouds after the base and also, it increases the likelihood of extra form drag, wave drag or boundary layer separation on the shrouds themselves. It seems likely that the extra drag is mostly coming from these effects on the shrouds themselves.

To return to the effects of boattail angle, it is clear that further tests e.g. with $\beta = 10^{\circ}$, $\theta = 10^{\circ}$, are really required before one can be dogmatic as to what is the correct explanation of the results presented here. Nevertheless, it seems probable that partly at least, one is observing an inevitable effect of changes in β. This would accord with general experience. Before this research, it was generally concluded that the boattail angle should be as high as possible, the limits being set by wave drag at supersonic speeds or the risk of boundary layer separation at subsonic speeds. Typical values in practice have been in the range 10° - 15° for supersonic speeds or 15° - 20° for subsonic speeds An important lesson from the study of the present results however is that one should not quote maximum values of β without regard to other parameters. On the second explanation above, an increase in β gives a higher base pressure but the risk of boundary layer

separation depends on the required pressure rise from the peak suction to the base. Hence, an increase in base pressure is acceptable and desirable provided the peak suction can also be reduced by an appropriate choice of boattail shape or as noted earlier, by designing for appropriate interference fields from other parts of the aircraft. What can be achieved as a good boattail shape will depend on various factors e.g. the values of b/m, j/m and (m - b)/L. As an example, it could be argued that the optimum value of β and the improvement in changing from $\beta = 10^{\circ}$ to $\beta = 15^{\circ}$ might be greater for the larger value of j/m. This appears to be confirmed by the results in fig.11a although, in view of the quoted standards of accuracy and repeatability, one would hesitate before making too much of this comparison.

5.3. Effect of Base Area

The base area was varied by progressively filling in the valley between the nozzles on the twin-jet configuration with $\beta = 15^{\circ}$. An increase in base area was therefore coupled with a reduction in the longitudinal rate of change of cross-sectional area along the boattail, as can be seen from fig.5. The base area ratios tested were b/m = 0.0407, 0.0685 (semi-filled valley) and 0.0963 (fully-filled valley); tests were made with two shroud area ratios of s/j = 1.0 and 1.7 In addition, the boattail with the smallest base area was tested with a fairing between the shrouds terminating at the nozzle exit plane; this configuration can be considered to have no base (i.e. b/m = 0); it is shown in the photograph in fig.7b.

The afterbody drag at typical operational jet pressure ratios for the range of base areas tested is shown in fig.15. The increase in base area obtained by filling in the valley between the nozzles gives an increase in C_{DA} that does not depend significantly on shroud ratio or Mach number at subsonic speeds but at M = 1 3, there is no noticeable change in drag between the semi- and fully filled cases. The effects on the individual pressure drag components at M = 0.7 is shown in fig.16. One important result is that the combined boattail and base drag remains constant, thus suggesting that the pressure and cross-sectional area changes tend to compensate; this can be confirmed by looking at the transverse pressure distributions at station 4 in the valley and on the base as shown in fig.17. The increase in base area leads, at subsonic speeds, to a poorer pressure recovery on the base and this is transmitted to the external shroud surfaces and the secondary duct exits and it is these changes that give rise to the substantial increase in C_{DA} with base area. Thus, a change in the boattail geometry, which is the responsibility of the airframe designer, results in a change of drag

on the external surface of the nozzles whose shape is traditionally, the responsibility of the engine designer. These results therefore highlight the importance of consultation and integration and the need for tests on the complete installation in order to optimise the drag. Tests on the nozzle without the boattail afterbody could be misleading.

The results with the internozzle fairing were disappointing. Figure 15 shows that in general, it did not give any reduction in drag relative to what was obtained with the standard base b/m = 0.0407. An oil flow test revealed the presence of a separation covering about a third of the area of the fairing. This is probably the explanation for the lack of continuous pressure recovery on the fairing as shown in the results in fig.17. This pressure recovery improves however in the presence of the jet. Despite this flow separation, a comparison of the mean pressure on the fairing with the base pressure without the fairing, fig.18, indicates an improved pressure recovery of about $\Delta C_p = 0.048$ at M = 0.7. Assuming that the external shroud surfaces adjacent to the base are affected similarly, this implies a reduction in C_D of about 0.005 which combined with a slightly lower contribution (0.002) from the boattail would imply an overall reduction in C_{DA} of 0.007 due to the fairing. This was not observed in the balance data but this could be an occasion where the accuracy of these data is not sufficient for an accurate comparison.

The apparently disappointing results with the internozzle fairing should not therefore be allowed to detract from the thesis that one should if possible try and reduce the afterbody drag by minimising the base between the nozzles. An inter-nozzle fairing may still be the correct solution provided care is taken to avoid a boundary layer separation on the fairing.

5.4. Single Jet: Effect of Boattail Lengths

Although the investigation of the effect of boattail length was not a principal aim of the test series, a comparison is possible from the tests on the two single jet configurations. The standard configuration had the same length as the twin-jet afterbodies but for the "short single", the boattail length was reduced to 0.633 of the full length bodies. This was to obtain a link with R.A.E. research on axisymmetric configurations with this shorter length. As noted earlier, the overall length of the "short single" was the same, a parallel section having been interposed ahead of the boattail. The comparison is for j/m = 0.13, s/j = 1.3, zero base and a boattail angle of $\beta = 15^{\circ}$.

Figure 19 shows that the comparison is very sensitive to whether the support interference corrections have been applied or not. This was discussed

earlier in Section 4.1. Having applied the corrections, the penalty due to reducing the length over which the body was boattailed varies from about 0.007 in C_{DAI} at subsonic speeds to 0 033 at M = 1.3. Before correcting for support and body interference, the penalty in C_{DA} at M = 1.3 was only 0.022. It is apparent from these results that differences in drag due to major changes of area distribution should be evaluated with proper regard to installation effects, not only in the test rig but also in the full-scale aircraft.

The pressure plotting results from these particular tests are not presented here. It appears however that the pressure recovery achieved at the base was almost the same for the two boattail lengths. This suggests that the higher drag at subsonic speeds with the shorter boattail was not due to a boundary layer separation but to extra form/friction drag associated with the greater suctions near the start of the boattail. It follows that if the shorter length could be combined with a different boattail shape or with favourable interference with some other part of the aircraft in order to avoid the higher suctions, one might find only a small penalty or even possibly an advantage from the shorter length. As an example, steep boattailing far aft and located behind the trailing edge of a fin or tailplane might be viewed favourably. It should be stressed once again that the comparison presented in this note was made for a specific purpose and was not intended as a major contribution to research into the effects of boattail length.

5.5. Variation with Effective Base Area

The results discussed above in Sections 5.1 and 5.3 have shown that afterbody drag increases with both shroud area ratio and base area and this suggests that one should consider the effect of the total projected area over which the external flow is necessarily separated. This effective total base area was estimated for each of the configurations tested and is illustrated in Fig.20. The effective base area, B, was taken to include the base area proper, b, the secondary duct annulus, s - j, and part of the external shroud surface bounded by the base and shroud exit. This last component was assumed, as shown in fig.20, to consist of sectors of 100°, 130° and 170° for b/m = 0.0407, 0 0685 and 0.0963 configurations respectively for j/m = 0 13 and 86° for the j/m = 0.07 configurations.

The afterbody drag coefficients for all the test configurations (with a shroud angle of 15°) at their representative operational jet pressure ratios are shown plotted against effective base area in fig.21. It is clear that particularly at the lower test Mach numbers and the associated lower jet pressure ratios, this concept of an effective base area over which the external flow is necessarily separated has considerable success in correlating the data for the majority of the configurations. In particular, it affords a means of reconciling the results for the single-jet and twin-jet afterbodies of the same boattail length.

The general trend is for C_{DAI} to increase linearly with B/m with a slope of 0.12. At M = 0.7, all the results with two exceptions lie in a band of width $\pm$0.004 in C_{DAI} around a mean line with this slope. Almost the same standard is maintained up to M = 0.95 but at M = 1.3, the correlation is not so successful because there is then relatively little variation in C_{DAI} with shroud area ratio for the single-jet afterbody and only a small drag penalty for the twin afterbody with the largest base area

There are two exceptions

(i) the "short single" afterbody for which the higher suctions at the start of the boattail give values of C_{DAI} that are about 0.006 above the mean variation for the standard length boattails,

and (ii) the twin-nozzle afterbody with zero base area created by adding an interfairing between the nozzles for which presumably as a result of the observed flow separation on the fairing, the values of C_{DAI} are perhaps 0.008 above the mean trend.

Within the band covering the rest of the data, one can detect various changes discussed earlier, e.g. the somewhat higher values of C_{DAI} at subsonic speeds with $\beta = 10^{o}$ as compared with $\beta = 15^{o}$.

Another feature of fig.21 calling for comment is the different apparent variation with Mach number in the results for the two sizes of jet. It should be noted that at a given jet pressure ratio, there is little variation in afterbody drag with Mach number between M = 0.7 and M = 0.95. The apparent variation in fig.21, i.e. a tendency for C_{DAI} to increase with M for the smaller jet and to decrease for the larger jet, is primarily due to the associated change in jet pressure ratio with Mach number. The data for the smaller jet, j/m = 0.07, are presented for higher jet pressure ratios than those for the larger jet, j/m = 0.13, in order to provide a comparison for a constant net thrust for engines of different bypass ratio. For the smaller jet, P_J/P varies from 3.2 at M = 0.7 to 5.1 at M = 0.95 while for the larger jet, the variation is from 2.1 to 3.4. The significant point is that broadly speaking, these two ranges lie on opposite sides of the jet pressure ratio at which C_{DAI} is a maximum relative to P_J/P - see fig.9. This explains the different apparent trends with Mach number. Also, incidentally, one should perhaps resist the temptation to compare the results for the two sizes of jet at the same base area. With the smaller jets, it should be possible to fair the boattails to a smaller base area thus giving a reduction in afterbody drag.

The comment was made in the introduction to this report that prior to this research programme, there had been a suspicion that the drag of a twin-jet

afterbody was usually higher than for the corresponding single-jet afterbody of the same base area. It has now been shown that for configurations of Class I with the afterbody terminating near the nozzle exits, this point has been resolved by the introduction of this concept of an effective base area. For a given true base area, the effective base area will always be larger for the twin-jet afterbody and this is evidently the main reason why the afterbody drag is higher.

6. CONCLUDING REMARKS

This report has summarised the main results from the first phase of a research programme into the drag of twin-jet afterbodies. All the configurations tested were in Class I i.e. with the afterbody terminating near the nozzle exits. Parameters investigated in the programme include jet size, base area with the changes obtained by infilling the valley between the nozzles and by extending as a fairing, afterbody boattail angle, nozzle shroud area ratio coupled with changes in shroud length as for a translating shroud, and shroud angle. Tests were made at Mach numbers from M = 0.7 to M = 0.95 and at M = 1.3 over a range of jet pressure ratios.

The accuracy of the final values of afterbody drag coefficient, C_{DAI}, based on fuselage cross-sectional area is thought to be about $\pm$0.004 corresponding to $\pm$10% of afterbody drag at subsonic speeds or $\pm$0.0004 as an aircraft C_D. In practice, it has been possible to recognise some differences smaller than this when they are obtained consistently in systematic comparisons.

Support interference was discussed in some detail in Section 4.1. Corrections have been applied to afterbody drag, these corrections are trivial at M = 0.7-0.8 and are thought to be known with adequate accuracy for all the Mach numbers of the present tests. However, the user of the data should consider possible interference effects due to the wings and fin-tail unit of his aircraft on the boundary layer and supercritical flow development on the boattailed afterbody which may possibly, according to the design of the aircraft, invalidate the "design rules" from the present test results.

At subsonic speeds and likely operational jet pressure ratios, the afterbody drag coefficient based on fuselage cross-sectional area lie in the range 0.03 - 0.06 of which typically, 0.026 can be ascribed to skin friction. Under these conditions, much of the variation in afterbody drag between different configurations can be expressed as a linear increase with a parameter known as effective base area that has been introduced to represent the area over which the external stream is necessarily separated. This effective base area includes the base area proper, the secondary duct annulus area and part of the external shroud

surface bounded by the base and the shroud exit. In particular, the concept appears to be a means of reconciling the drag of single- and twin-nozzle installations of the present type with the nozzle exits close to the base. The rate of increase of afterbody drag with effective base area is given by 0.12 x B/m. At M = 1.3, or at higher jet pressure ratios at any Mach number, this simple type of correlation is less successful.

The other main results include the following:

1. The increase in afterbody drag with shroud area ratio is greater for the larger jets and at the higher jet pressure ratios; it also depends somewhat on afterbody boattail angle,
2. An increase in shroud angle from 15° to 20° with a boattail angle of 15° increases the afterbody drag coefficient by 0.004 subsonically or 0.007 at M = 1.3,
3. A reduction in boattail angle from 15° to 10° is beneficial at M = 1.3 but gives a small penalty subsonically due to a poorer pressure recovery at the base being transmitted onto the shroud surfaces,
4. An attempt to reduce the drag by means of an internozzle fairing to give zero base area was unsuccessful but this does not detract from the idea in principle; it merely means that one should be careful to avoid the flow separation on the fairing which occurred in this case,
5. The reduction in boattail length for the single-jet afterbodies gave a substantial drag increment particularly at supersonic speeds but it is clear that such comparisons with major changes of area distribution have to be evaluated with proper regard to installation effects both in the test rig and in the full-scale aircraft.

A general conclusion from the test results is that they have demonstrated:

on the one hand, the need to evaluate nozzle designs from tests in which the boattailed afterbody is present,

and on the other hand, the need to establish corrections for jet effects, i.e. corrections to apply to test results for complete aircraft models with inadequate representation of the jets, from tests in which the nozzles are fully represented.

NOTATION

a	local cross-sectional area
b	base area (fig.3)
B	effective base area (fig.20)
C_D	drag coefficient based on maximum cross-sectional area, m.
C_{DA}	afterbody drag coefficient (uncorrected for forebody and strut interference) $= \left[X_{M=0} - (X - D)_M \right] \Big/ mq$ at measured $W\sqrt{T}$ and PJ/P
C_{DAI}	afterbody drag coefficient corrected for forebody and strut interference = $C_{DA} + C_{DI}$
C_{DAP}	afterbody pressure drag coefficient = $C_{D1} + C_{D2} + C_{D3} + C_{D4}$
C_{DF}	afterbody skin friction drag coefficient
C_{DI}	drag interference coefficient derived from cylindrical pressure distribution
C_{D1}	boattail pressure drag coefficient
C_{D2}	base drag coefficient
C_{D3}	shroud pressure drag coefficient
C_{D4}	secondary duct drag coefficient
C_p	pressure coefficient
$\bar{C}_{pb}$	average base pressure coefficient
$\bar{C}_{ps}$	average secondary duct pressure coefficient
j	combined exit area primary nozzles
L	length of boattailed section of afterbody (fig.5)
m	maximum cross-sectional area of model = 30.82 in^2
M	free stream Mach number
PJ/P	primary jet total pressure/free stream static pressure
q	free stream dynamic pressure
s	combined exit area of shrouds
$W\sqrt{T}$	mass flow x (jet total temperature)$^{\frac{1}{2}}$
x	distance from start of boattail
X	thrust
X-D	thrust minus drag = installed thrust
β	afterbody boattail angle
θ	external angle
ΔC_{DA}	afterbody drag coefficient increment

REFERENCES

1.	POZNIAK, O.M.	Afterbody Drag Measurements at Transonic Speeds on a Series of Afterbodies Terminating at the Jet-Exit. ARA MODEL TEST NOTE M.38/1. June 1972.
2.	POZNIAK, O.M.	Afterbody Drag Measurements at Transonic Speeds on a Series of Afterbodies Terminating at the Jet-Exit. PART II - Pressure results and jet-off force results. ARA MODEL TEST NOTE M.38/2. May 1972.
3.	MIGDAL, D. MILLER, E.H. SCHNELL, W.C.	An Experimental Investigation of Exhaust Nozzle/Airframe Interference. AIAA Paper No. 69-43. June 1969.
4.	RUNCKEL, J.F.	Aerodynamic Interference between Exhaust System and Airframe. AGARD CP71, paper 15. September 1970.
5.	LEE, E.E. RUNCKEL, J.F.	Performance of Closely Spaced Twin-jet Afterbodies with different inboard-outboard Fairing and Nozzle Shapes. NASA TM-X 2329. September 1971.
6.	CHESTERS, C.M. POZNIAK, O.M.	The Design and Development of a Rig for measuring the installed Performance of Twin Nozzle Afterbodies. Paper presented at the 32nd SemiAnnual Meeting of the S.T.A. September 1969.
7.	CHESTERS, C.M.	Computer Programme for the Reduction of twin Nozzle Thrust Minus Drag Rig (B.15) Results. Rolls-Royce Ltd. Installation Research REPORT IAR 86011. April 1968.
8.	BERGMAN, D.	An Aerodynamic Drag Study of Jet Engine Nozzles. AGARD CP-91-71, paper 22. September 1971.
9.	BERGMAN, D.	Effects of Engine Exhaust Flow on Boattail Drag. AIAA Paper No. 70-132. January 1970.

TABLE

I CONFIGURATIONS TESTED

Type of nozzle	j/m	β	b/m	Shroud area / jet area	s/j	Shroud Angle Deg.
Twin	.07	10	.0407	1, 1.3, 1.7, 2.1		15
"	"	15	"	" " " "		"
"	.13	10	"	" " " "		"
"	"	15	"	" " " "		"
"	"	"	"	1 - - -		20
" with interfairing	"	"	0	1 - - -		15
" semi-filled	"	"	.0685	1 - 1.7 -		"
" fully-filled	"	"	.0963	" - " -		"
Single	"	"	0	1, 1.3, 1.7, 2.1		"
Short single	"	"	"	- " - -		"
Single with conical plug	0	"	0	- - - -		"

II NOMINAL TEST CONDITIONS

Small jets, j/m = 0.07

M	PJ/p
0.7, 0.8	5, 4.5, 4, 3.5, 3, 2.5, 2, 1.5, 1
0.9, 0.95	6, 5.5, 5, 4.5, 4, 3.5, 3, 2.5, 2, 1

Large jets j/m = 0.13

M	PJ/p
0.7, 0.8	5, 4.5, 4, 3.5, 3, 2.5, 2, 1.5, 1
0.9, 0.95	6, 5.5, 5, 4.5, 4, 3.5, 3, 2.5, 2, 1
1.3	7, 6, 5.5, 5, 4.5, 4, 3.5, 3, 2.5, 2, 1

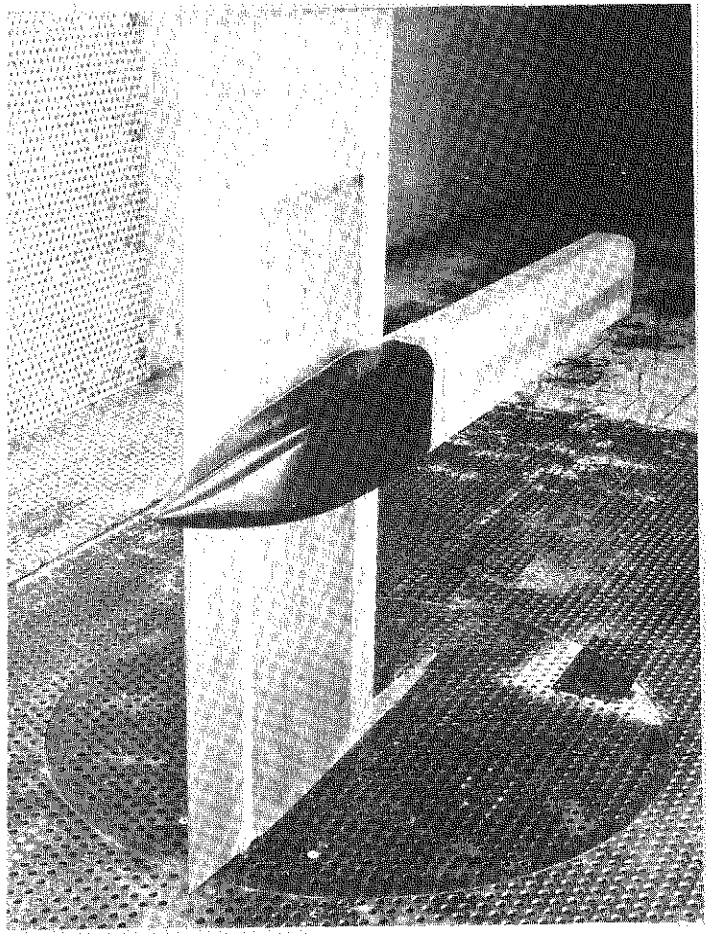

(a) FRONT VIEW WITH CYLINDRICAL AFTERBODY

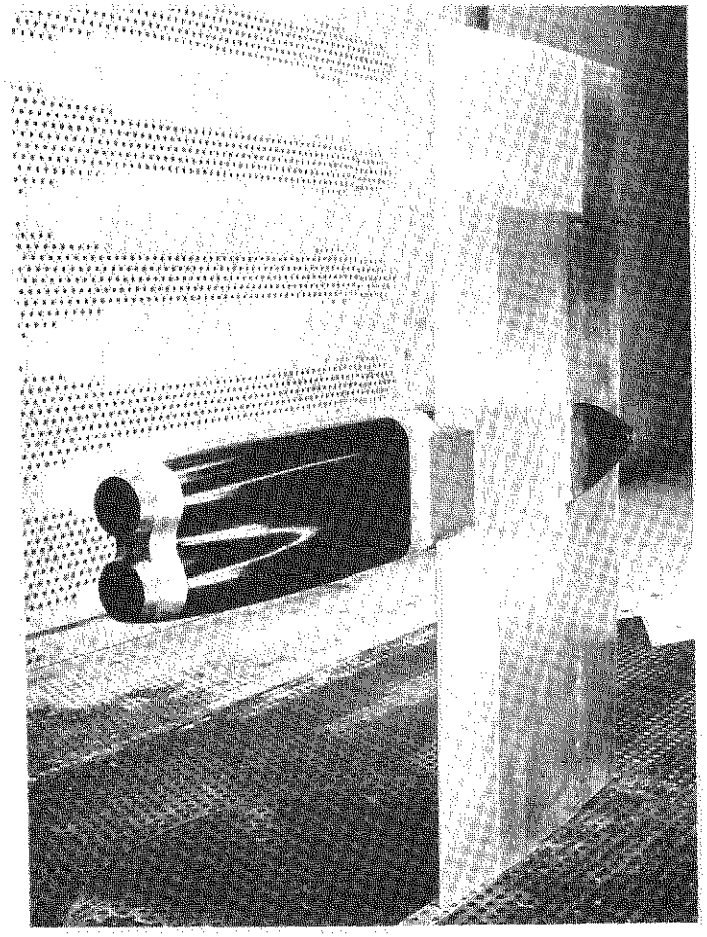

(b) REAR VIEW

FIG. 1

FIG. 1 MODEL INSTALLED IN A.R.A. TRANSONIC WIND-TUNNEL

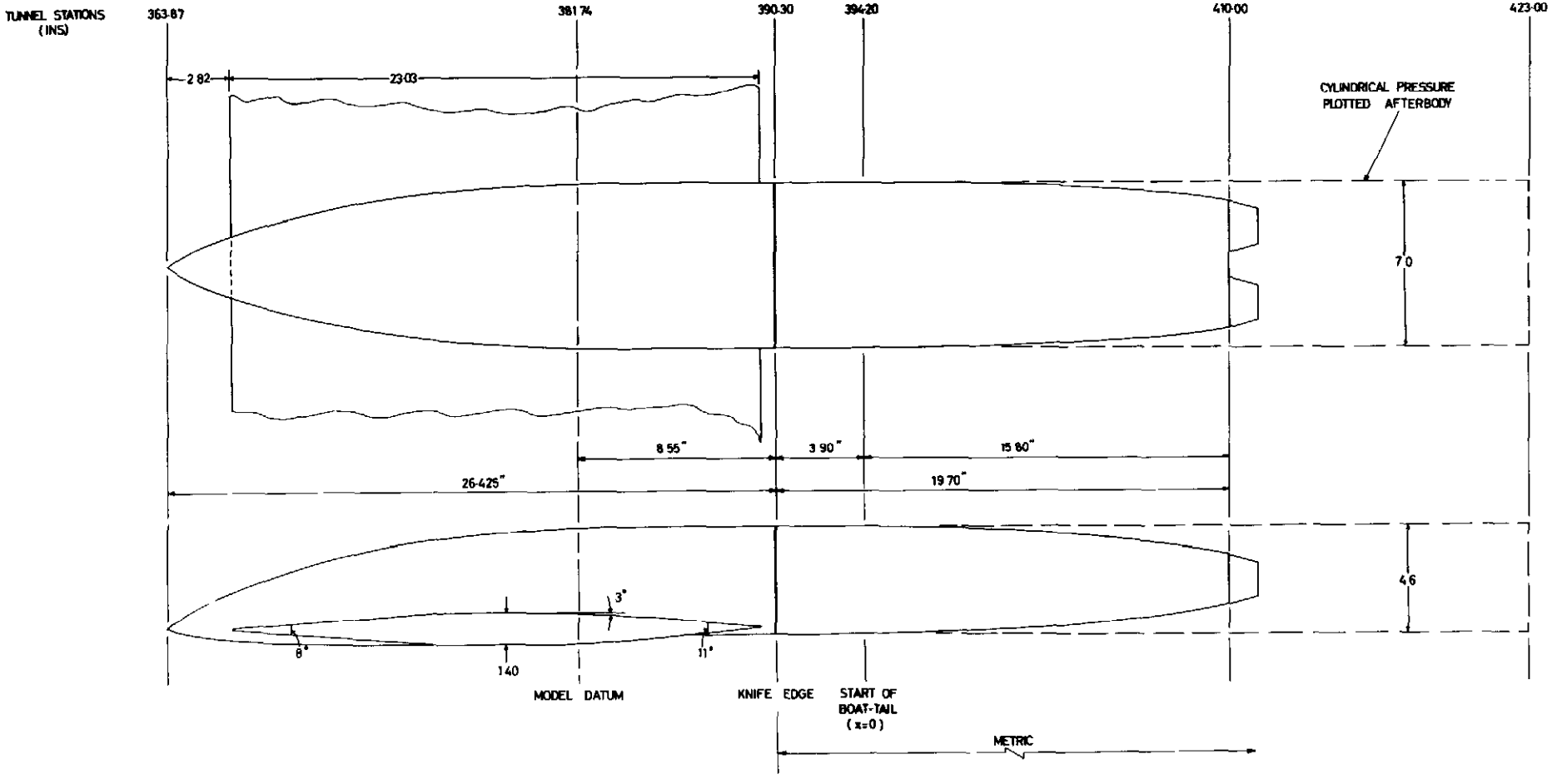

FIG. 2 MODEL DIMENSIONS AND LOCATION IN TUNNEL

FIG. 2

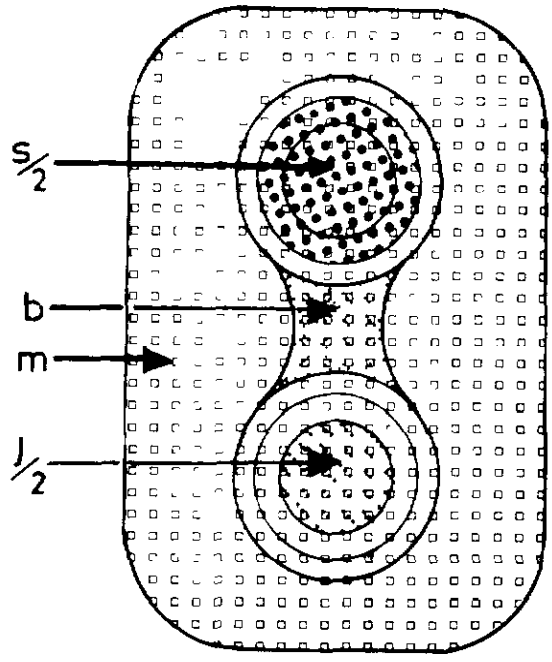

s = Exit area of shrouds
b = Base area
m = Maximum cross-sectional area
j = Exit area of primary nozzles

a. DEFINITION OF AREAS

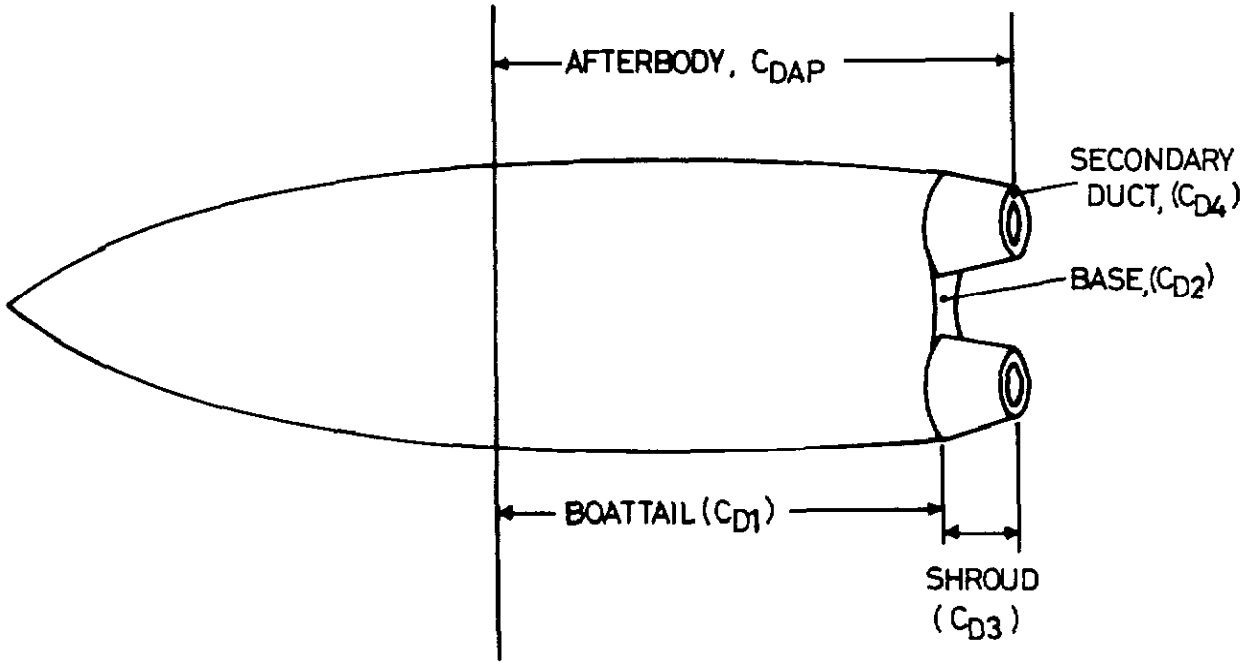

b. DESCRIPTIVE NOTATION WITH REFERENCE TO PRESSURE DRAG COMPONENTS

FIG. 3 DEFINITION OF AREAS AND DRAG COMPONENTS

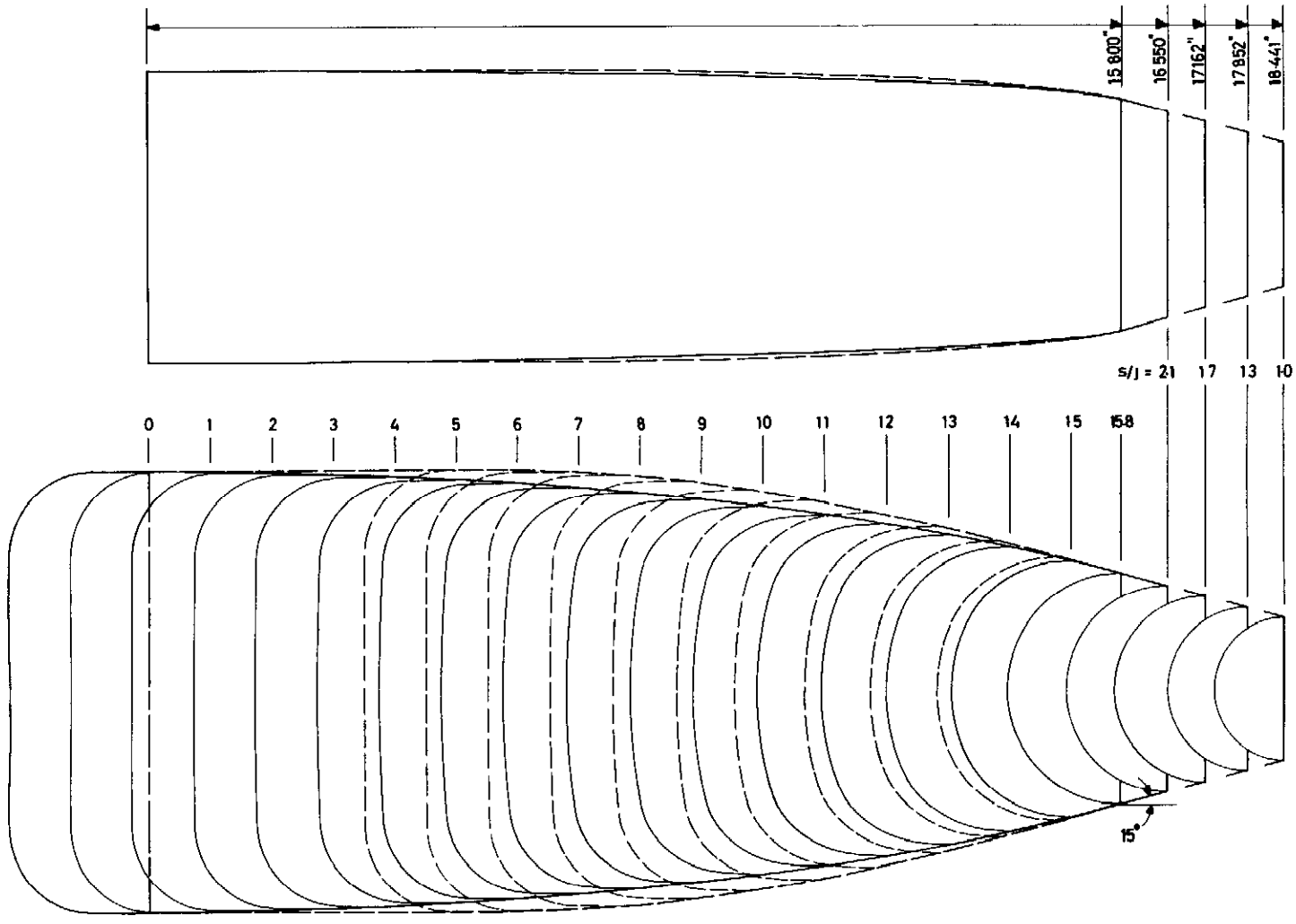

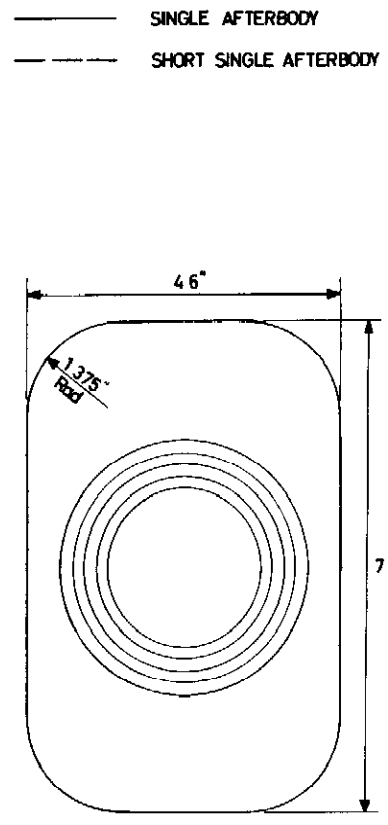

SINGLE AFTERBODY

SHORT SINGLE AFTERBODY

FIG. 4a

FIG. 4a DETAILS OF AFTERBODIES SINGLE & SHORT SINGLE

$j/m = 0.13 \quad b/m = 0 \quad \beta = 15^\circ$

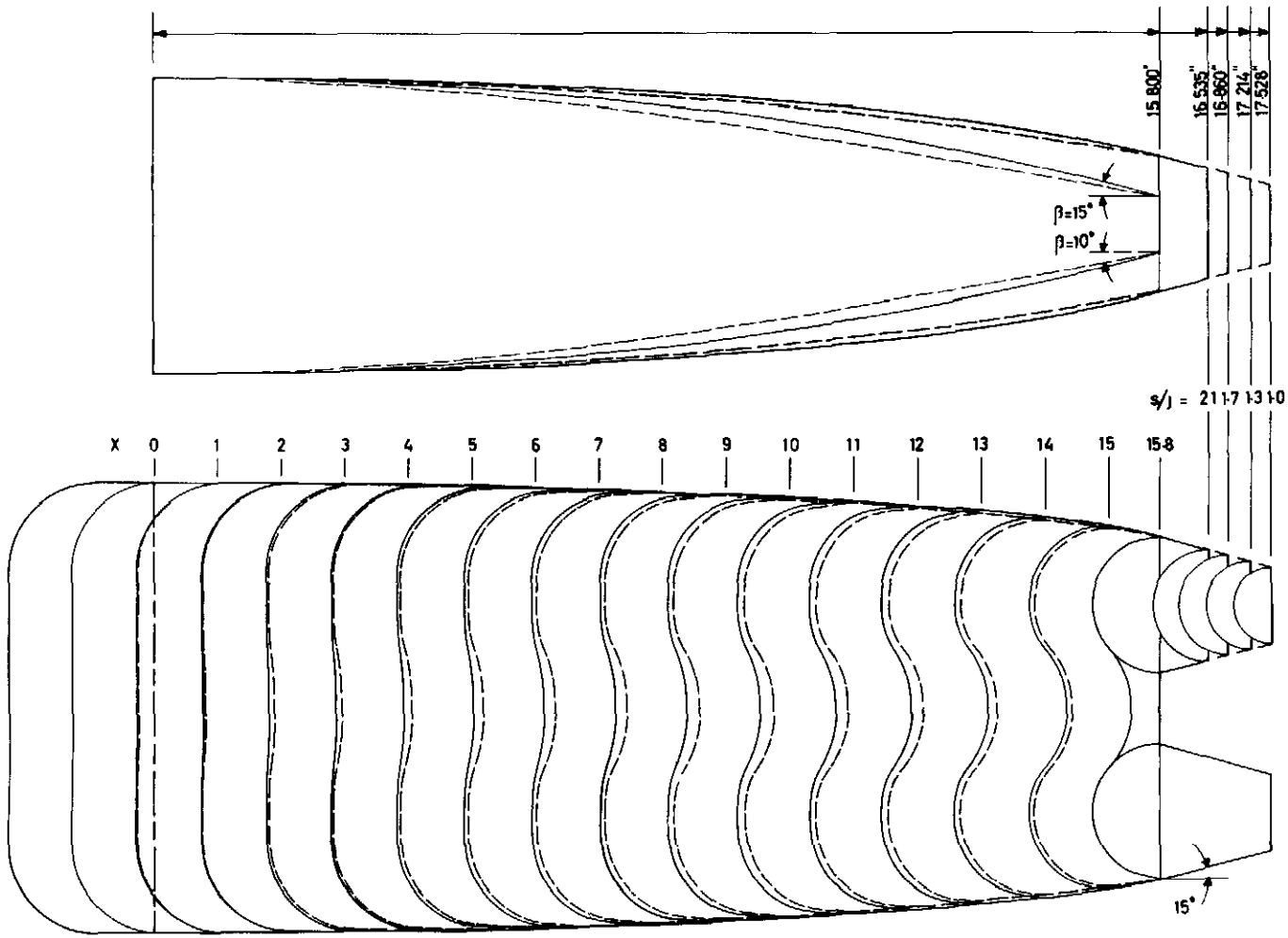

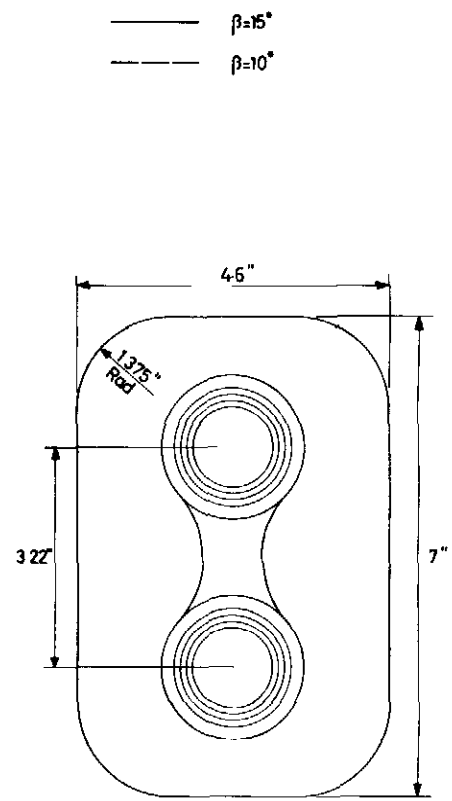

FIG. 4b

FIG. 4b DETAILS OF AFTERBODIES β=10° & 15°

j/m=0·07 b/m=0·0407

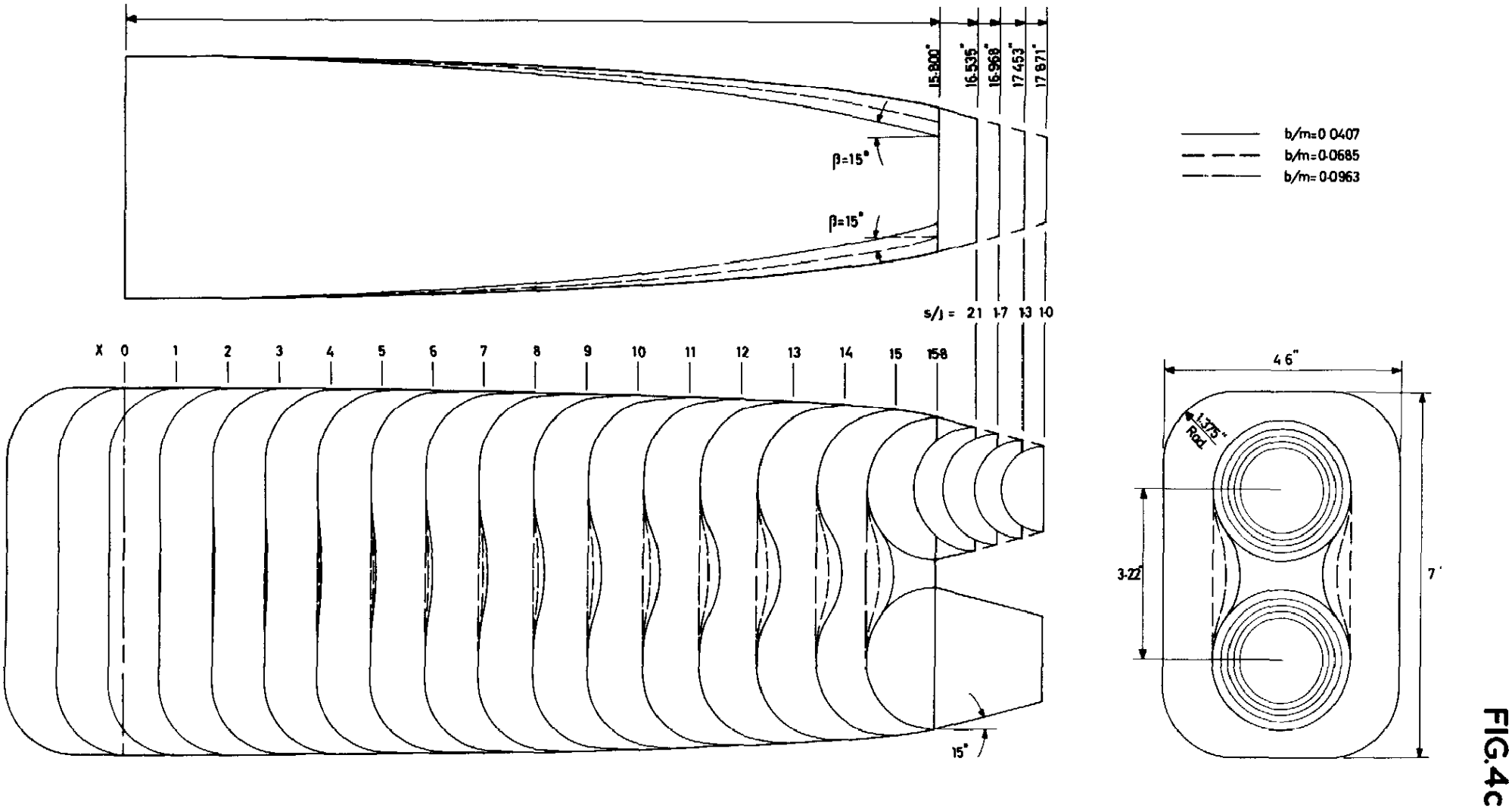

FIG. 4c

FIG. 4 c DETAILS OF AFTERBODIES b/m=0.0407, 0.0685 & 0.0963

j/m=0.13 β=15°

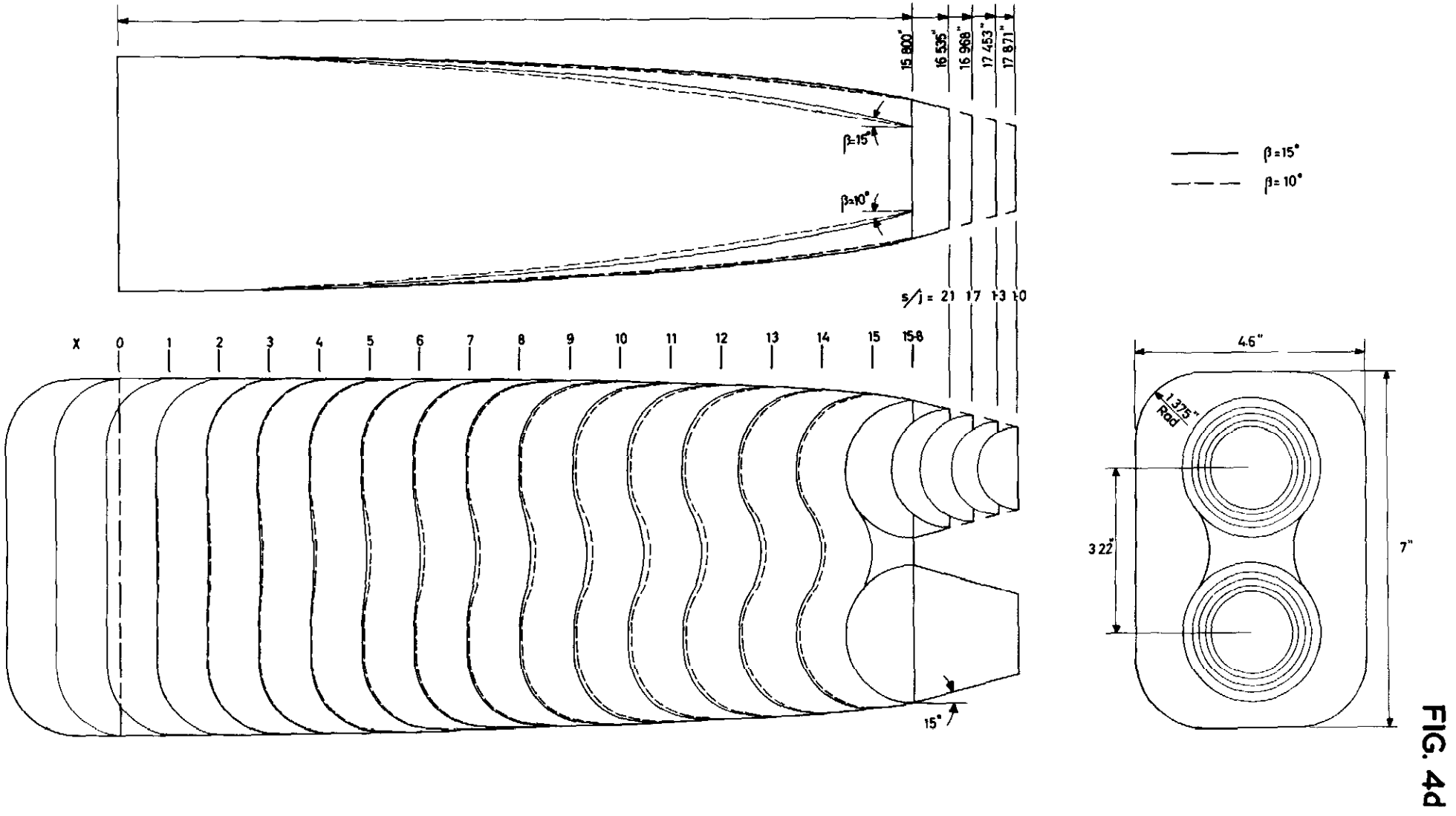

FIG. 4d

FIG. 4d DETAILS OF AFTERBODIES $\beta = 10° \& 15°$

$j/m = 0.13 \quad b/m = 0.0407$

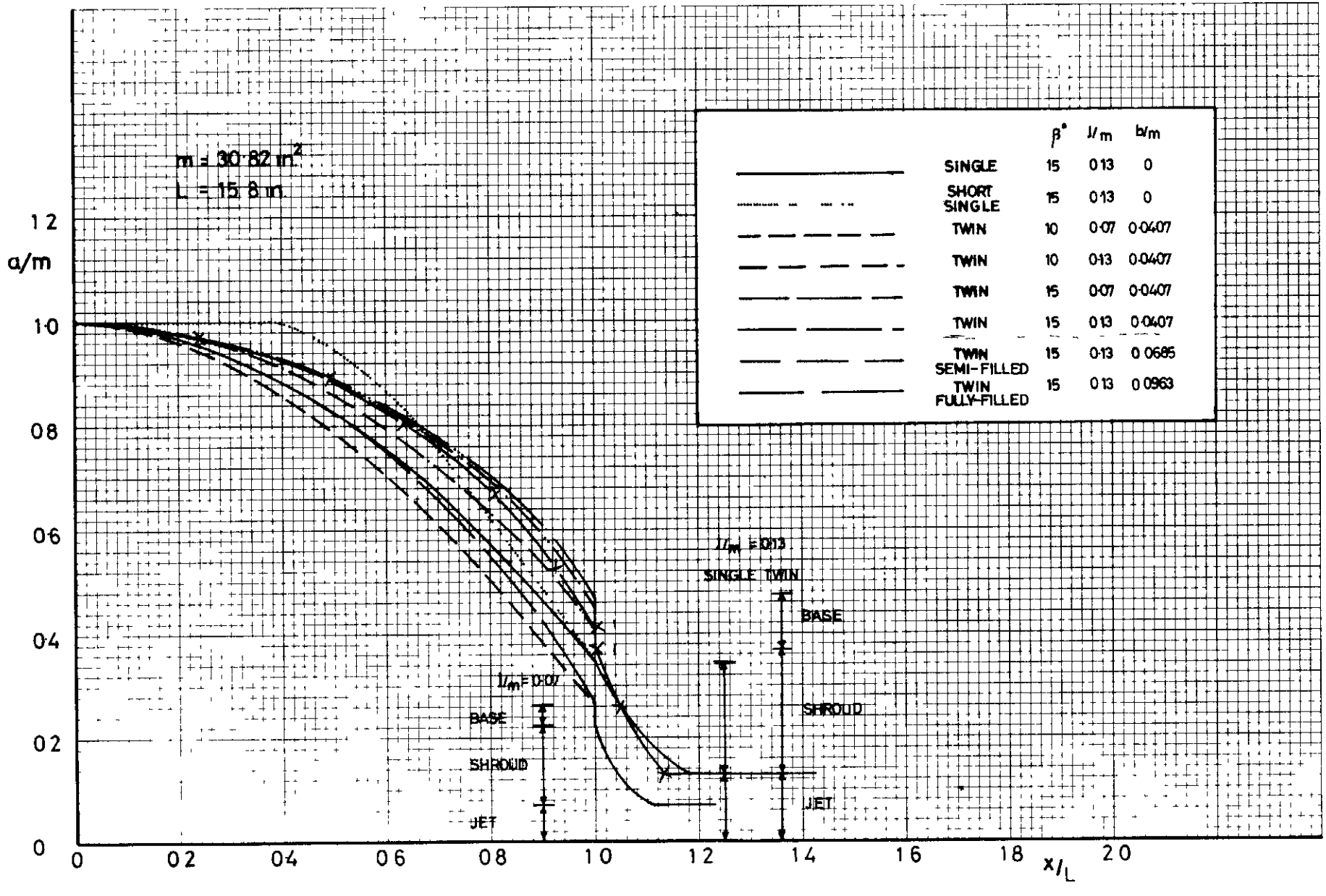

FIG. 5

FIG. 5 AREA DISTRIBUTIONS OF AFTERBODIES AND SHROUDS

FIG. 6

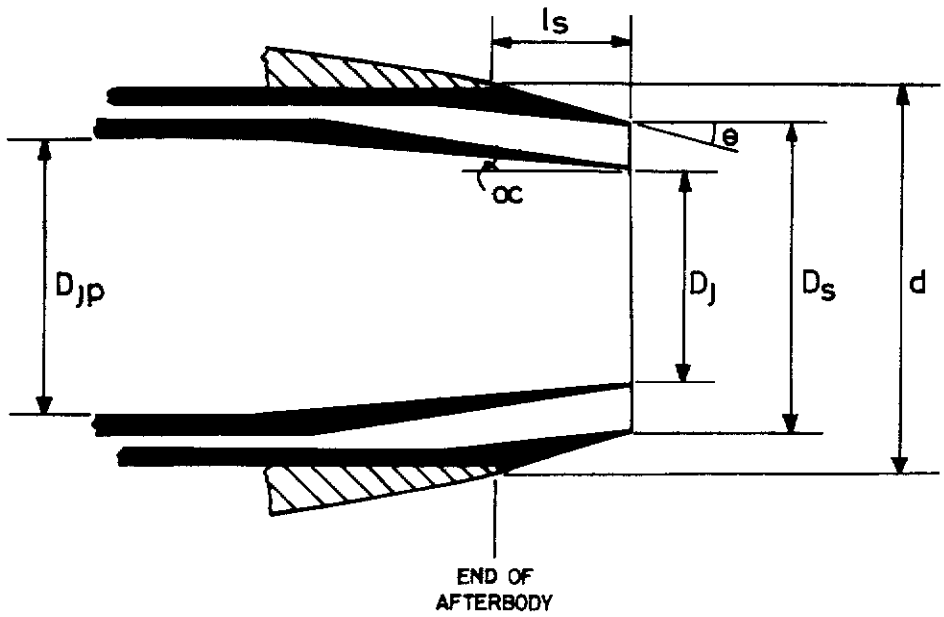

TYPE	j/m (nominal)	s/j	Djp (in)	Dj (in)	j (in²)	ls (in)	Ds (in)	s (in²)	d (in)	αc	θ
TWIN CONVERGENT	0 07	1 0	1 541	1 170	2 1503	1 728	1 186	2 210	2 110	5°-3'-36"	15°
"	"	1 3	"	"	"	1 414	1 353	2 876	"	"	"
"	"	1 7	"	"	"	1 060	1 543	3 740	"	"	"
"	"	2 1	"	"	"	0 735	1 715	4 620	"	"	"
"	0 13	1 0	2000	1 599	4·0187	2·071	1 165	4 097	2 722	5°-11'-13'	15°
"	"	1 3	"	"	"	1·653	1 835	5 289	"	"	"
"	"	1 7	.	"	"	1 168	2 096	6 901	"	"	"
"	"	2 1	"	"	"	0 735	2 327	8 506	"	"	"
TWIN, 20° SHROUD	"	1·0	"	"	"	1 522	1 615	4 097	"	"	20°
SINGLE CONVERGENT	0 13	1 0	2 828	2·252	3 9814	2 641	2 252	3 981	3 674	5°	15°
"	"	1 3	"	"	"	2 052	2 574	5 204	"	"	"
"	"	1 7	"	"	"	1 362	2 949	6·830	"	"	"
"	"	2 1	"	"	"	0 750	3 273	8 414	"	"	"

(N B FOR TWIN CONFIGURATIONS QUOTED AREAS ARE THE SUM OF BOTH NOZZLES)

FIG. 6 DETAILS OF NOZZLES AND SHROUDS

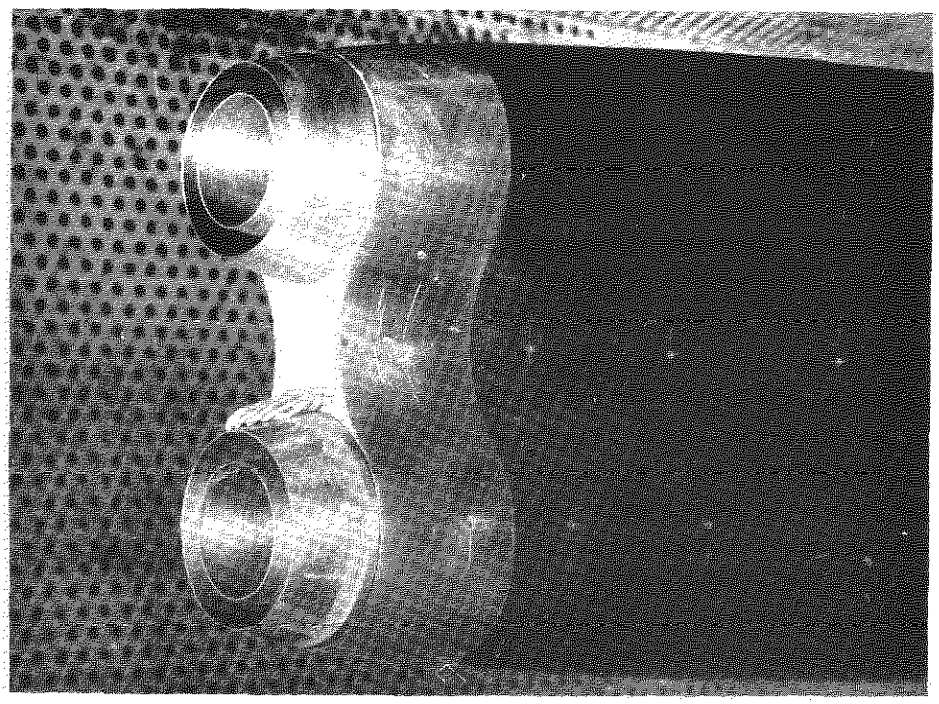

FIG. 7 (a.) TYPICAL NOZZLE SHROUD ASSEMBLY

(j/m=0·07 b/m=0·0407 s/j=2·1 β=15°, TWIN)

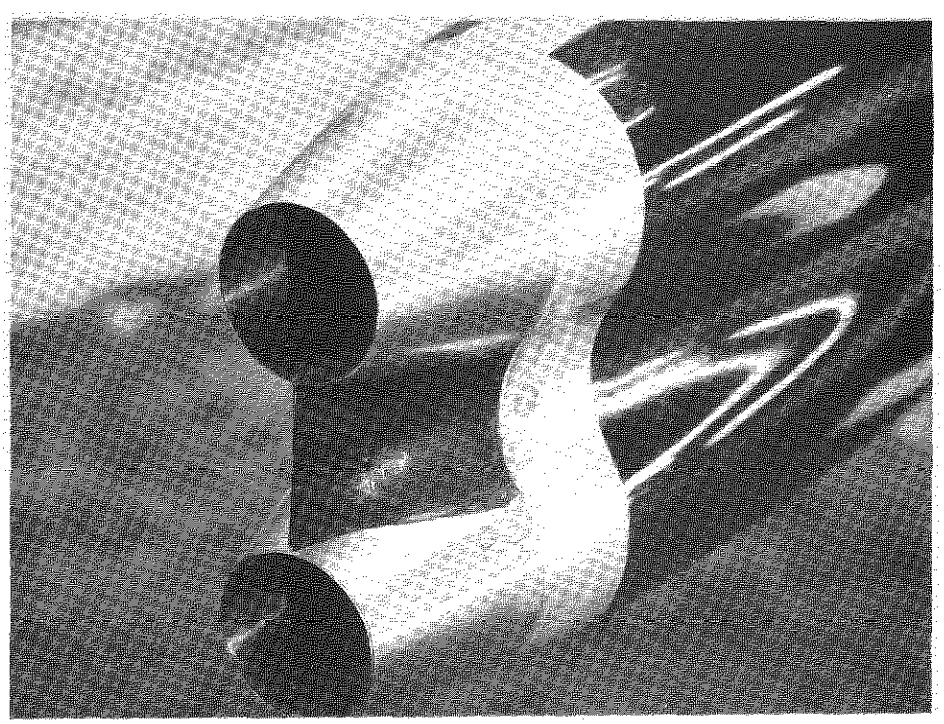

FIG. 7(b.) INTER NOZZLE FAIRING

(j/m = 0·13 b/m=0 s/j=1·0 β=15°, TWIN)

FIG. 8a

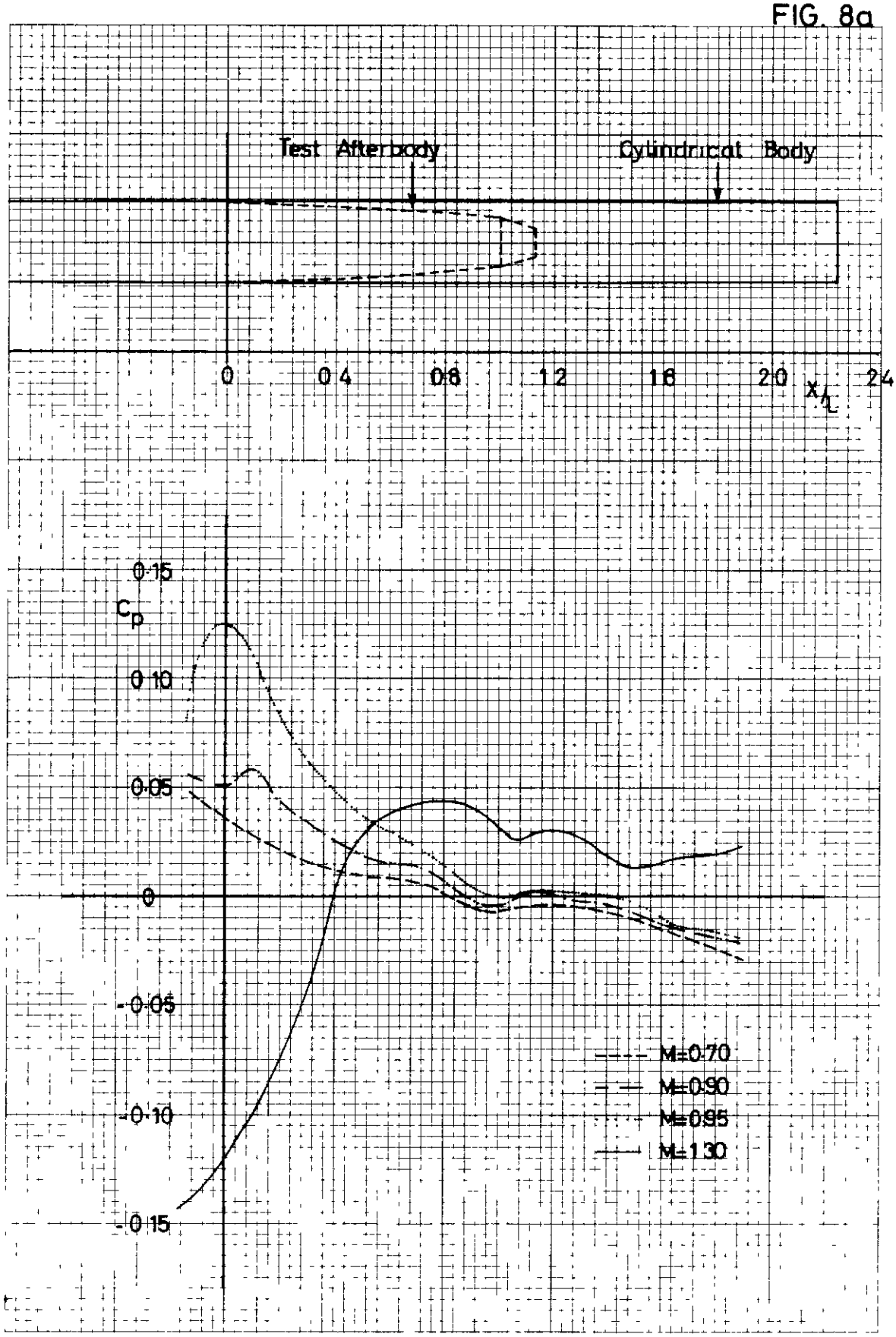

MEAN PRESSURE DISTRIBUTION ON CYLINDRICAL BODY

FIG. 8a SUPPORT INTERFERENCE

FIG. 8b

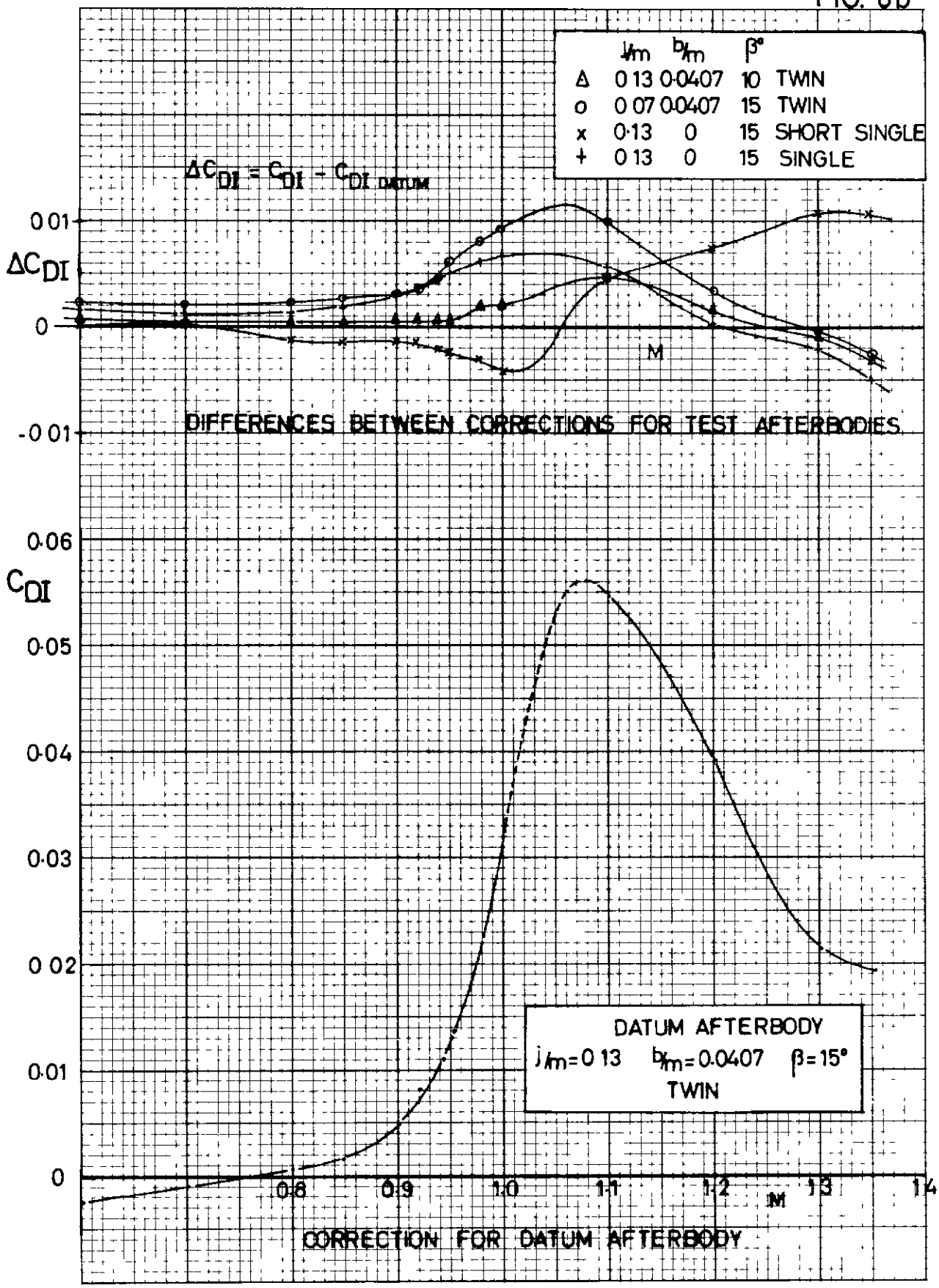

CORRECTIONS TO AFTERBODY DRAG

FIG. 8b SUPPORT INTERFERENCE

FIG. 8c

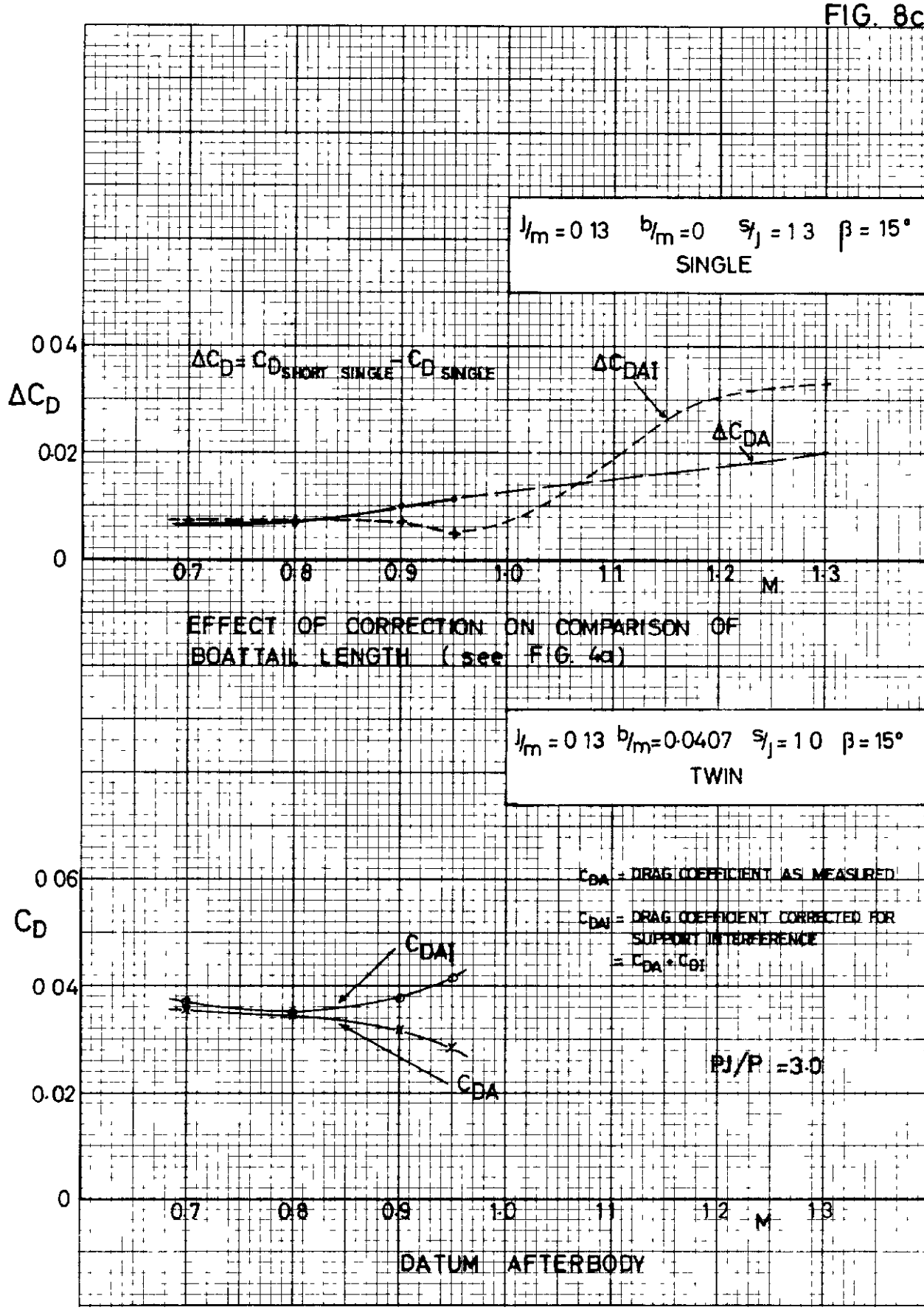

EFFECT ON VARIATION OF AFTERBODY DRAG WITH MACH NUMBER

FIG. 8c SUPPORT INTERFERENCE

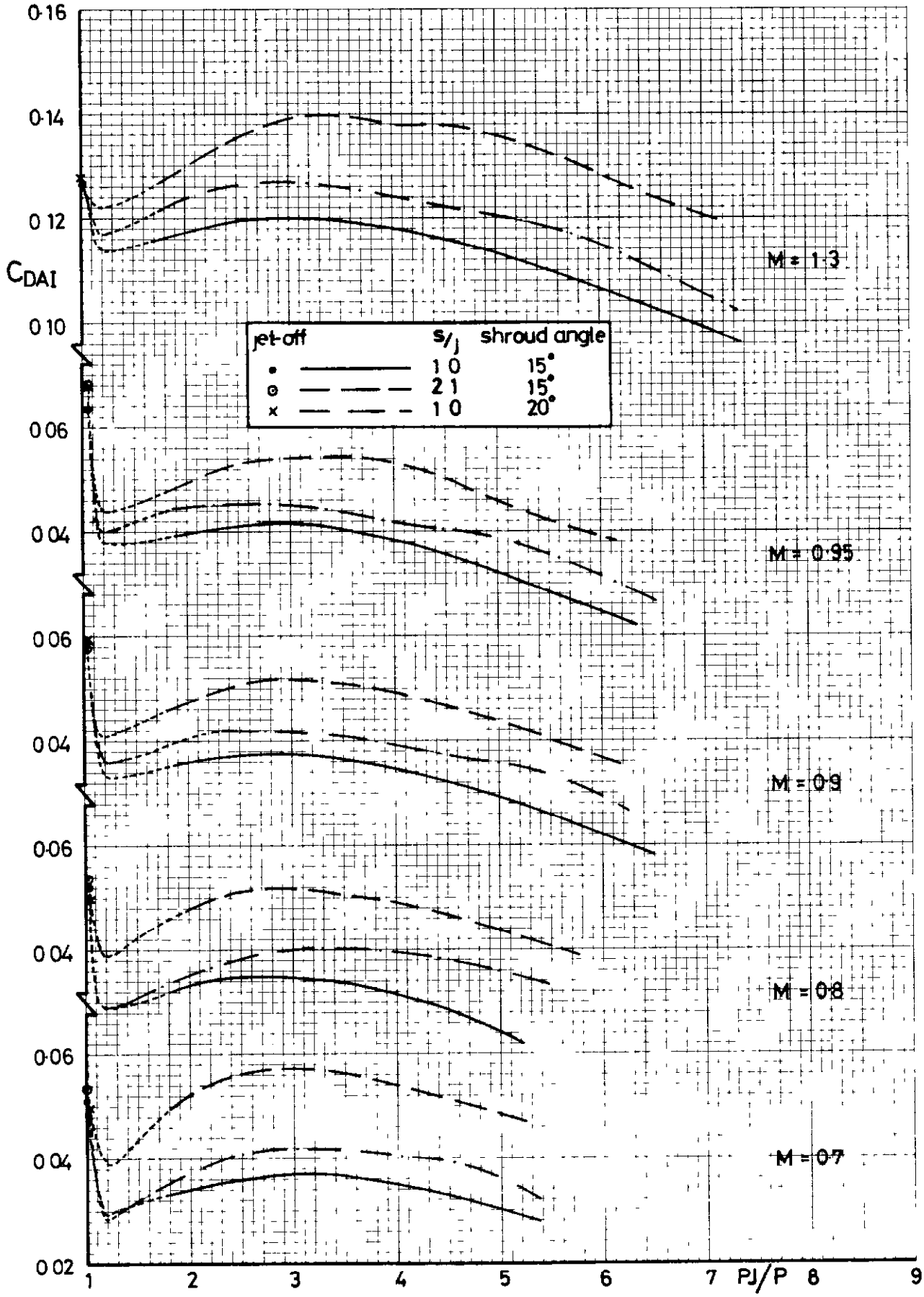

FIG. 9 AFTERBODY DRAG

EFFECT OF JET PRESSURE RATIO

FIG. 10

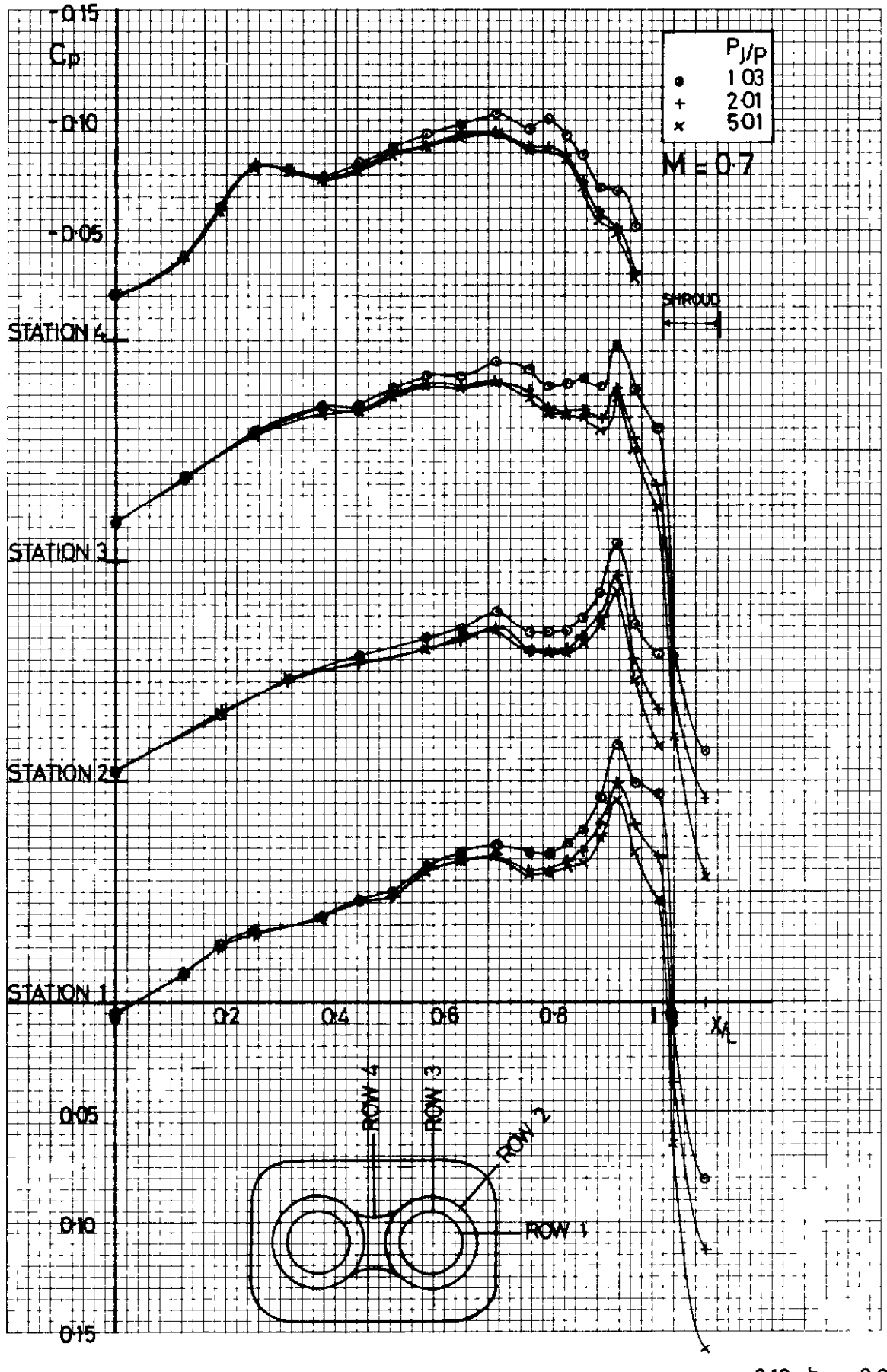

J/m = 0·13 $b_{/m}$ = 0·0407

$s_{/j}$ = 1·3 β = 15°

TWIN

FIG. 10 AXIAL PRESSURE DISTRIBUTION
EFFECT OF JET PRESSURE RATIO

FIG 11a

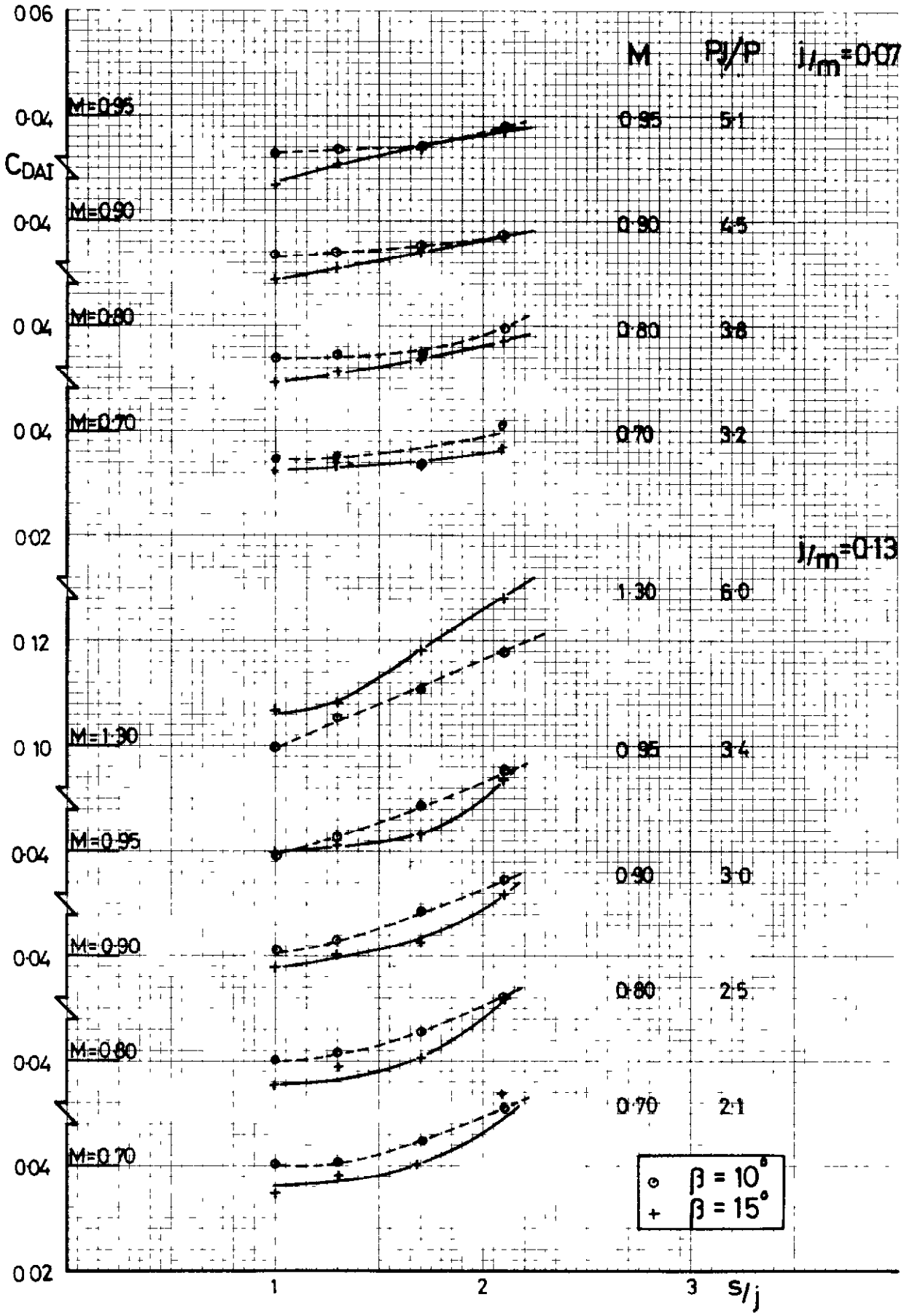

FIG 11a AFTERBODY DRAG $b/m = 0.0407$

EFFECT OF SHROUD AREA TWIN NOZZLE

FIG. 11b

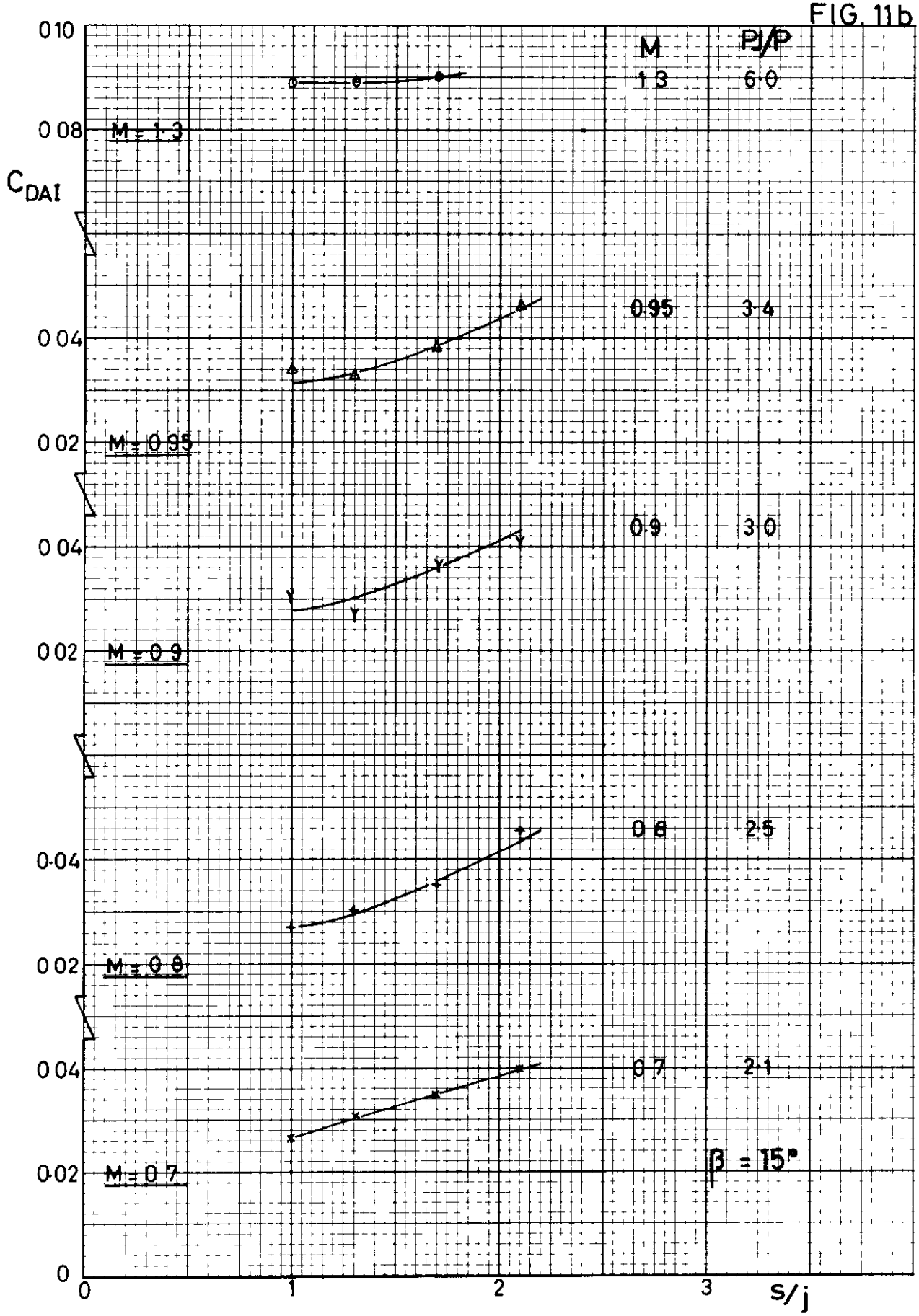

FIG. 11b AFTERBODY DRAG EFFECT OF SHROUD AREA

$j/_m = 0.13$ $b/_m = 0$
SINGLE NOZZLE

FIG. 12a

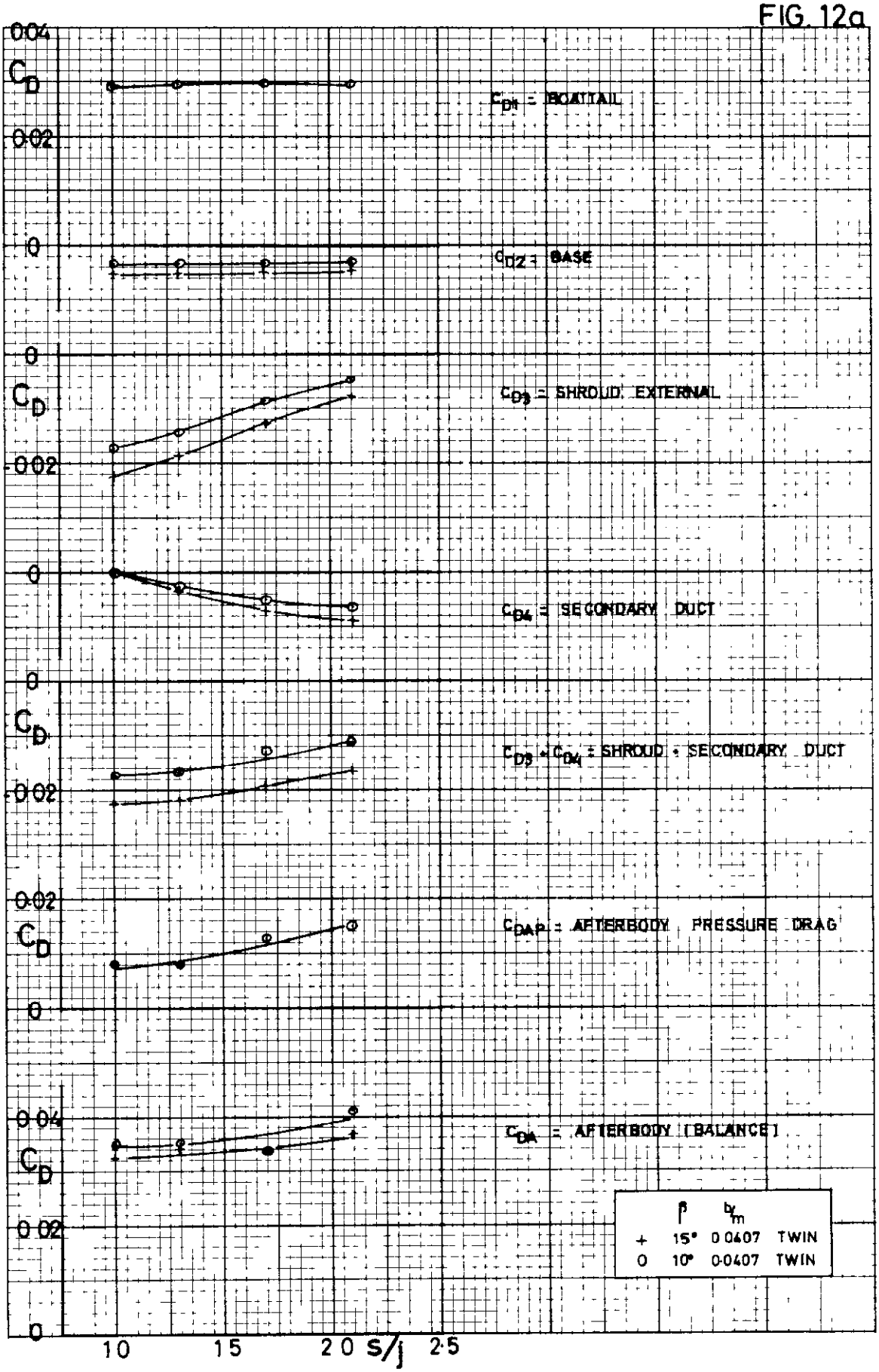

FIG. 12 a DRAG COMPONENTS

EFFECT OF SHROUD AREA AND BOATTAIL ANGLE

$M = 0.7$ $j/_m = 0.07$ $P_{j/_P} = 3.2$

FIG. 12b

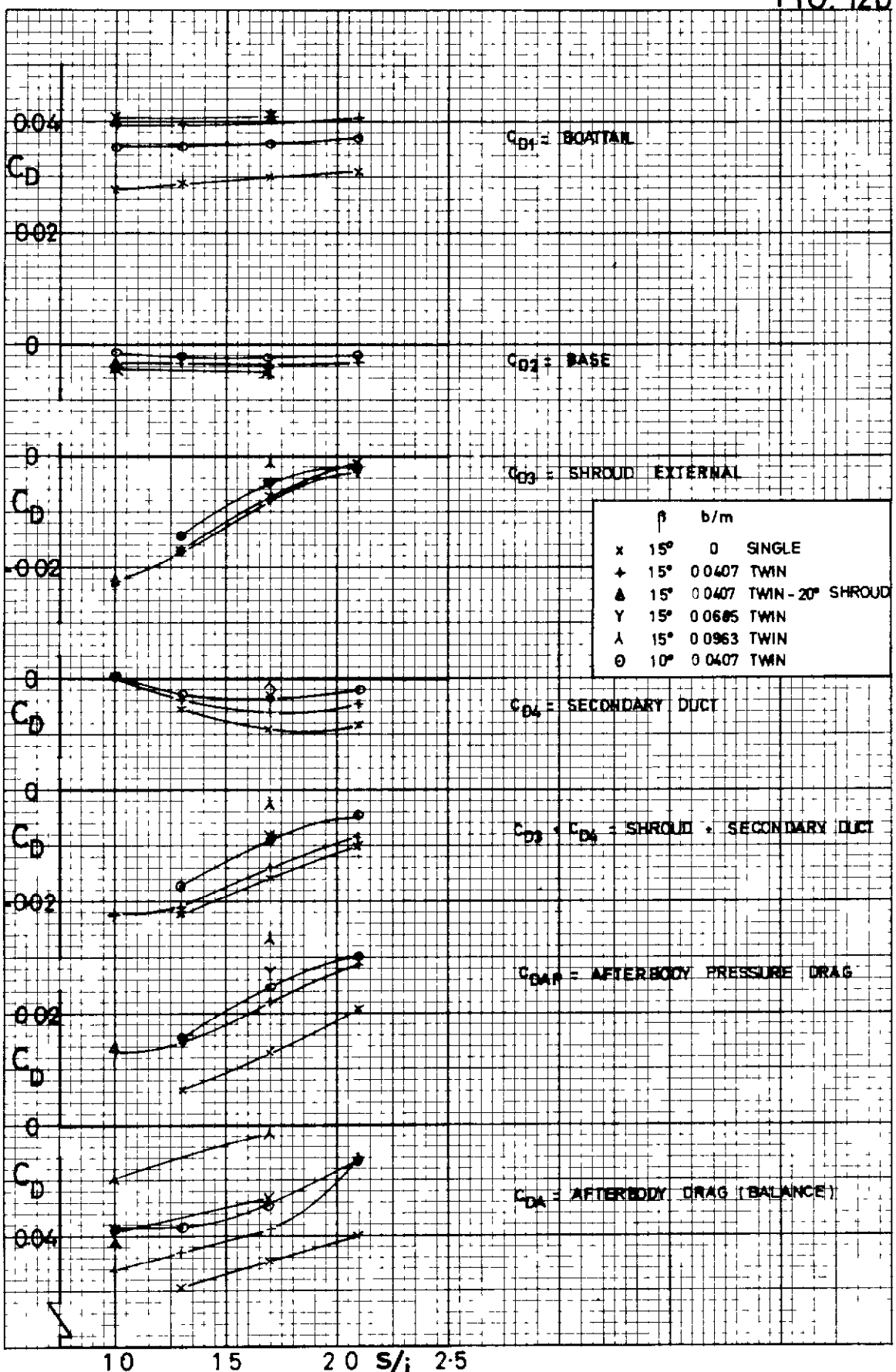

FIG. 12b DRAG COMPONENTS

EFFECT OF SHROUD AREA AND BOATTAIL ANGLE

$M = 0.7$ $j/_m = 0.13$ $P_j/_P = 2.1$

FIG. 13

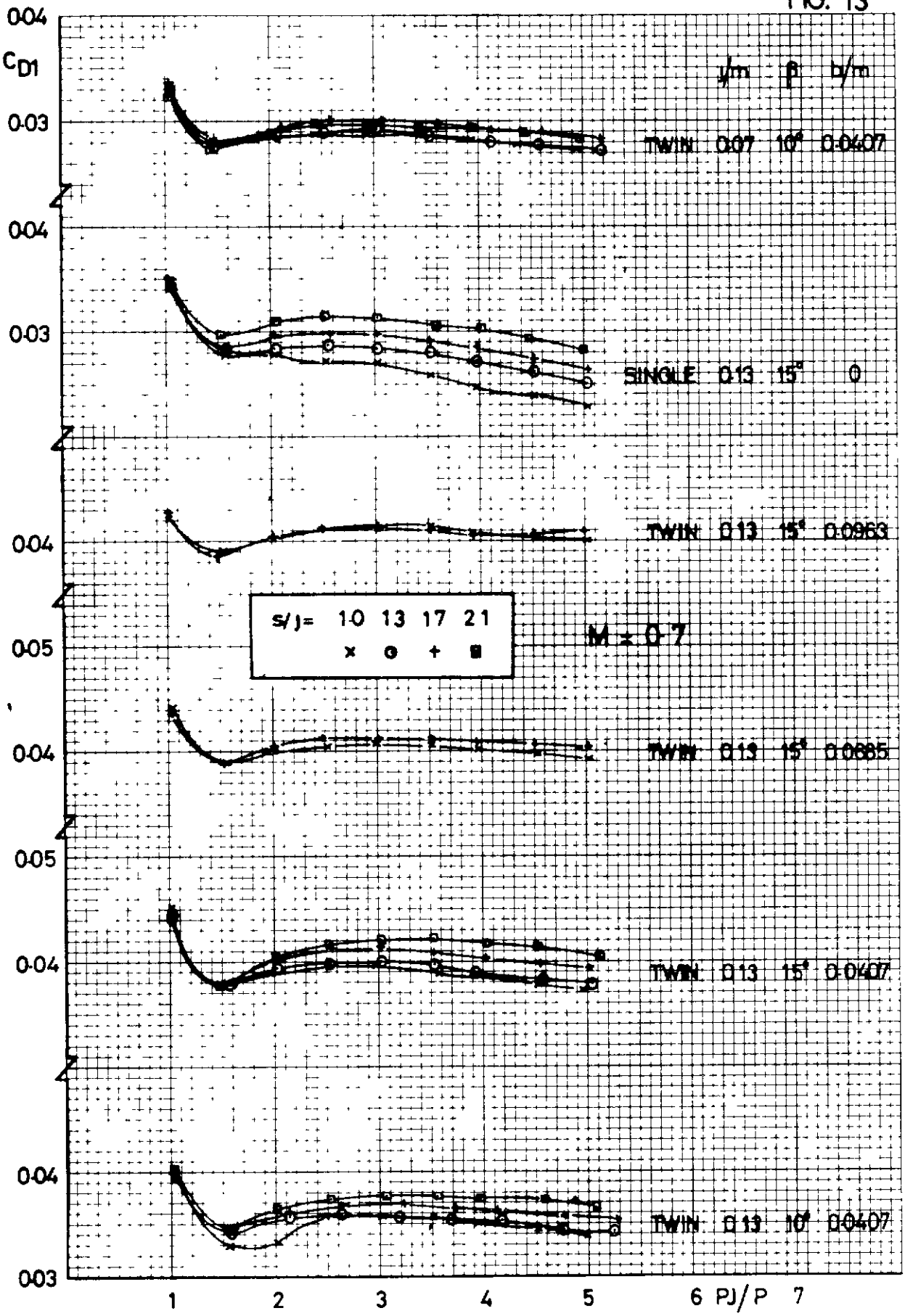

FIG. 13 BOAT TAIL PRESSURE DRAG

EFFECT OF SHROUD AREA

FIG. 14a

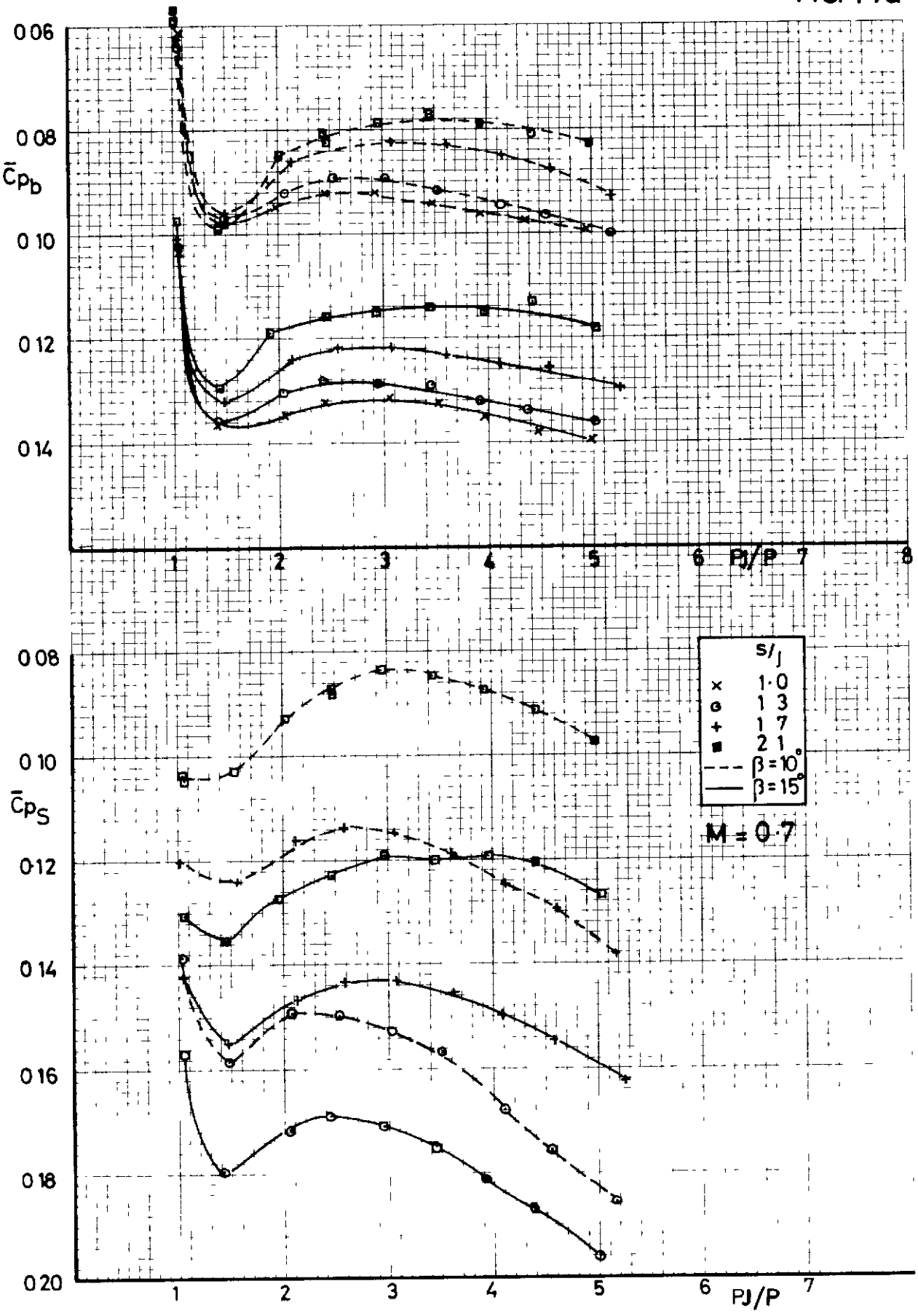

FIG. 14a BASE AND SECONDARY PRESSURE EFFECT OF SHROUD AREA ; $j/_m = 0{\cdot}07$

FIG 14b

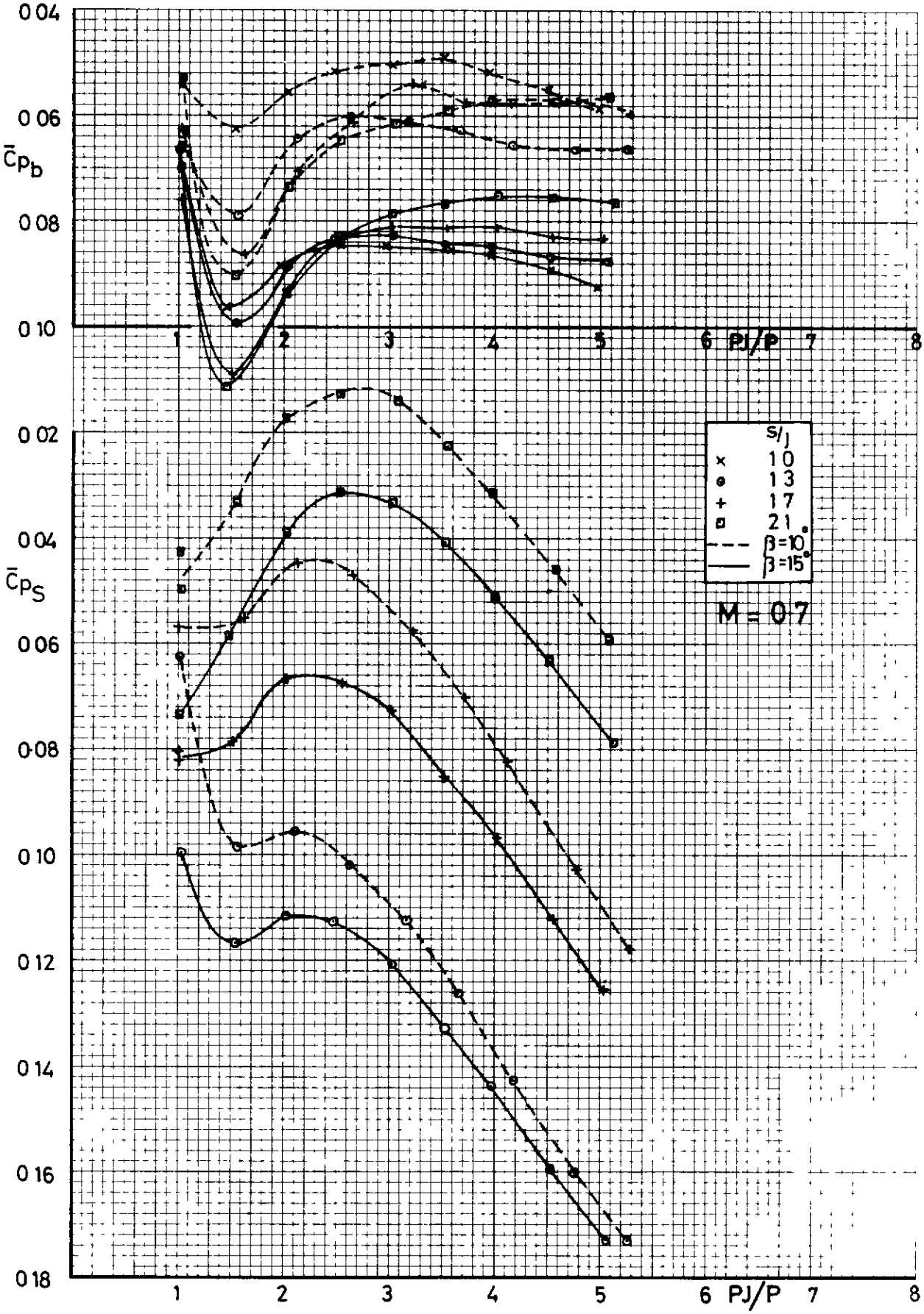

$b/_m$ = 0 0407 TWIN

FIG. 14b BASE AND SECONDARY PRESSURE EFFECT OF SHROUD AREA ; $J/_m$ = 0·13

FIG. 15

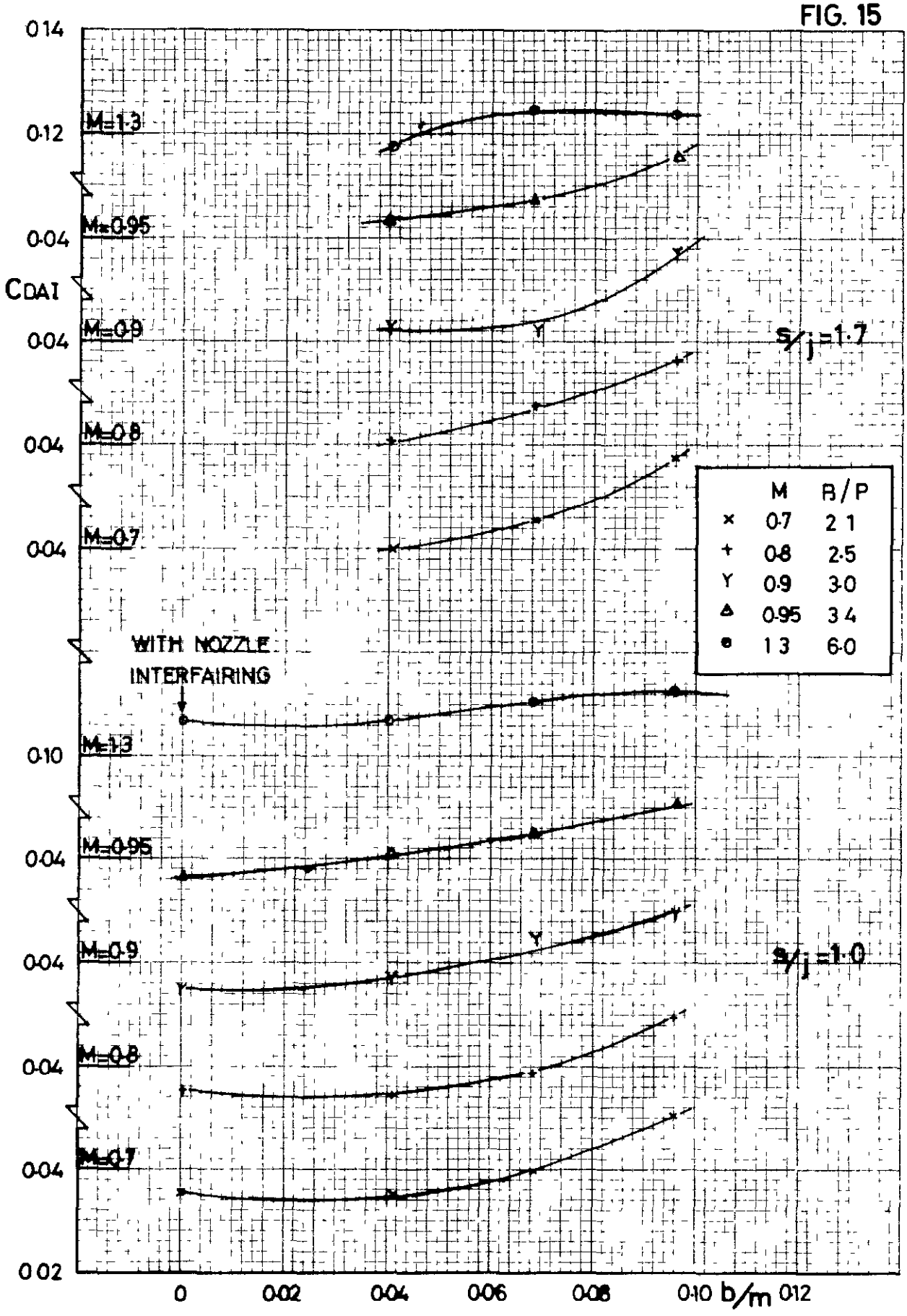

FIG. 15 AFTERBODY DRAG EFFECT OF BASE AREA

J/m=0·13 β=15°
TWIN NOZZLE

FIG. 16

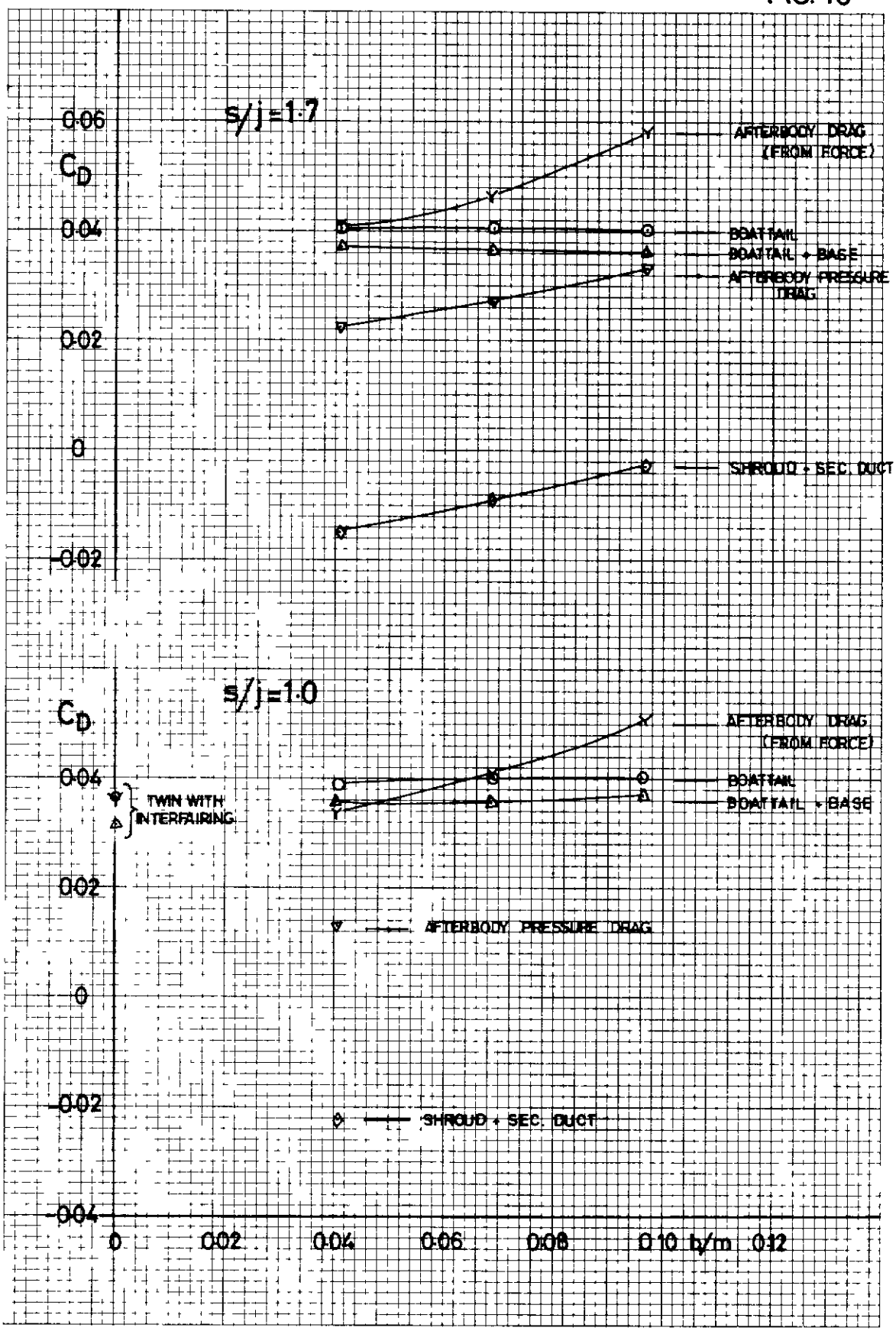

FIG. 16 DRAG COMPONENTS $\beta=15°$

EFFECT OF BASE AREA TWIN

$M = 0\,7 \quad j/_m = 0{\cdot}13 \quad P_{j/P} = 2\,1$

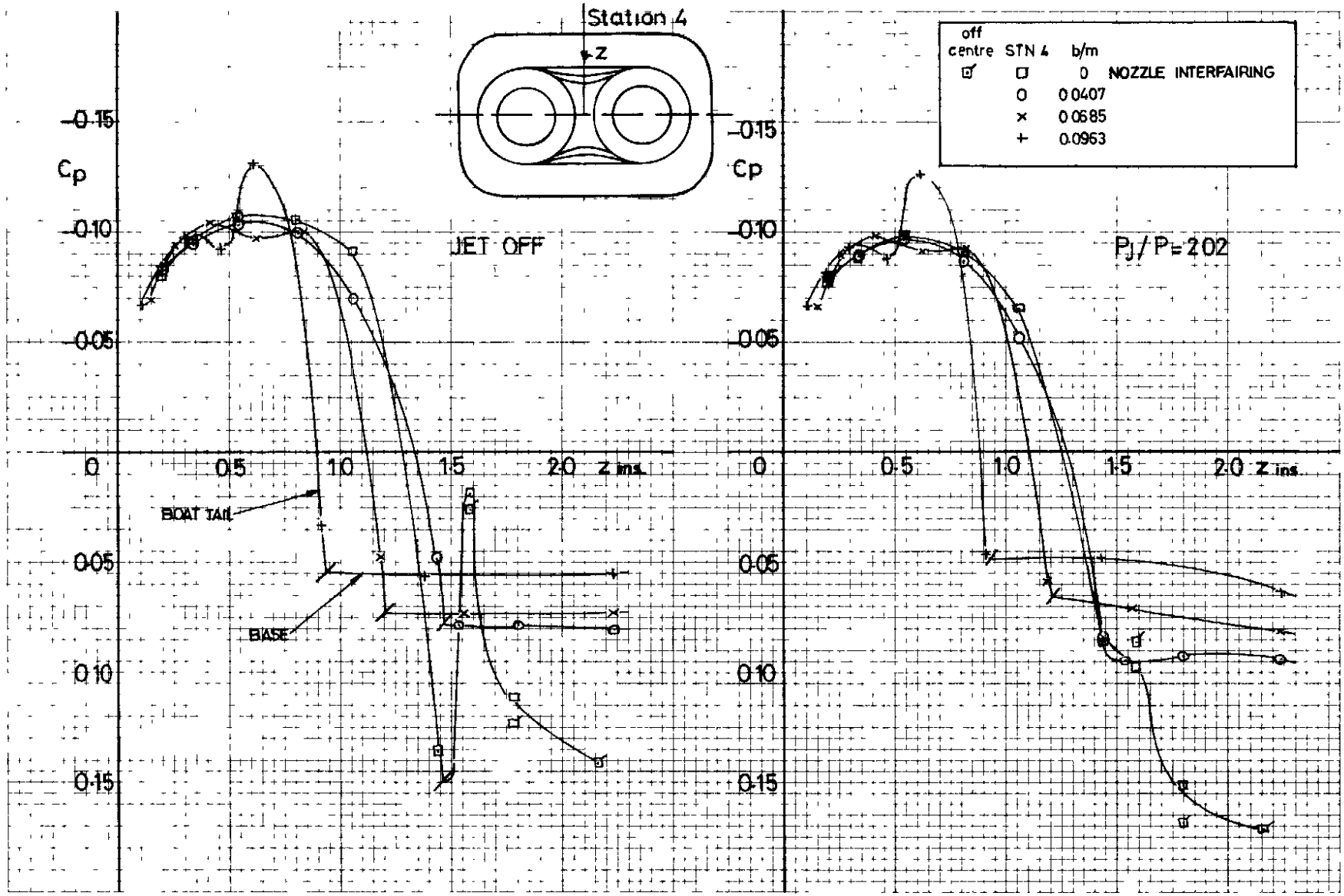

FIG. 17

FIG. 17 TRANSVERSE PRESSURE DISTRIBUTION STATION 4 j/m = 0.13 s/j = 1.0
EFFECT OF BASE AREA M=0.7 β = 15° TWIN

FIG. 18

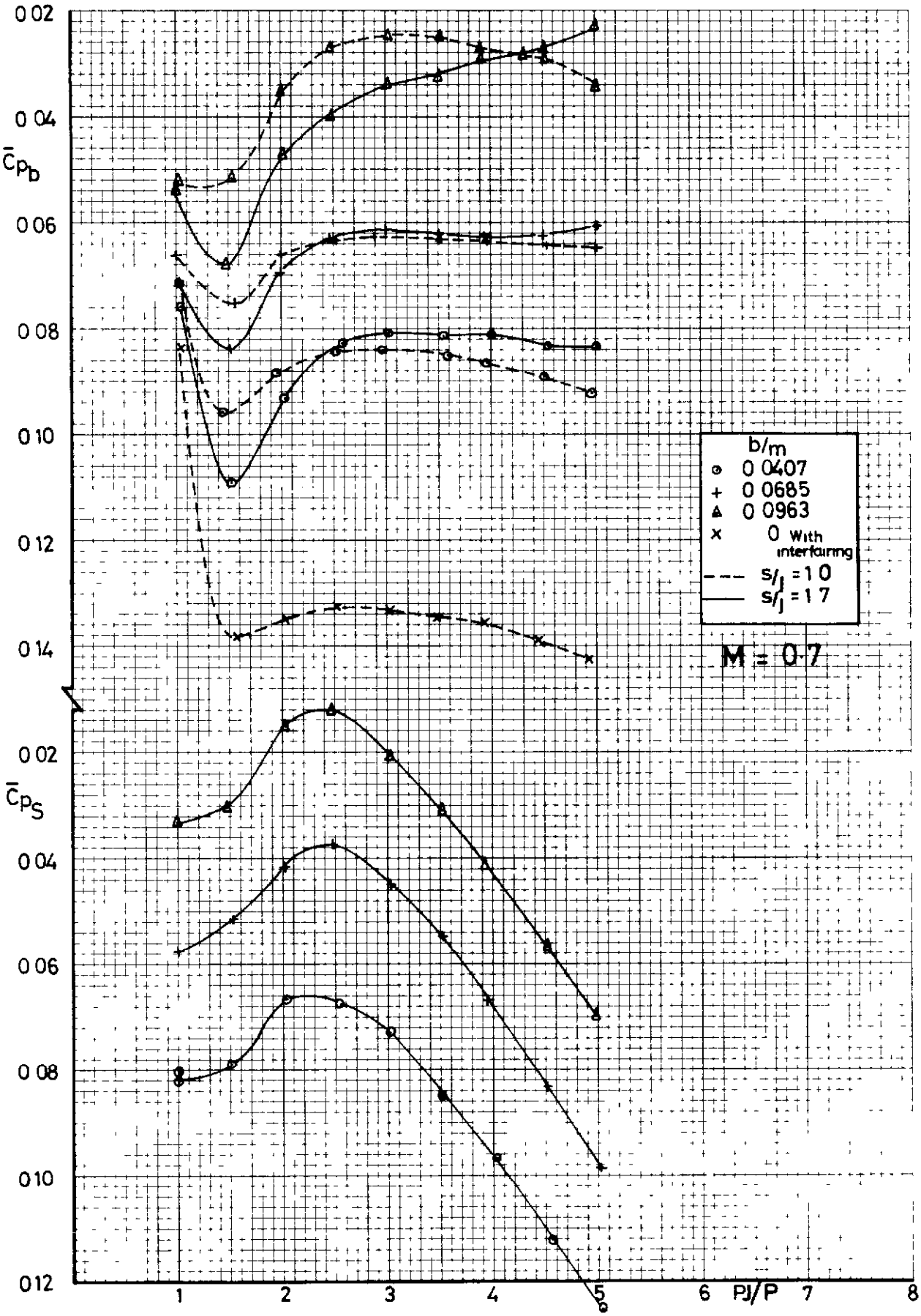

FIG. 18 BASE AND SECONDARY PRESSURE EFFECT OF BASE AREA

J/m = 0 13
β = 15°
TWIN

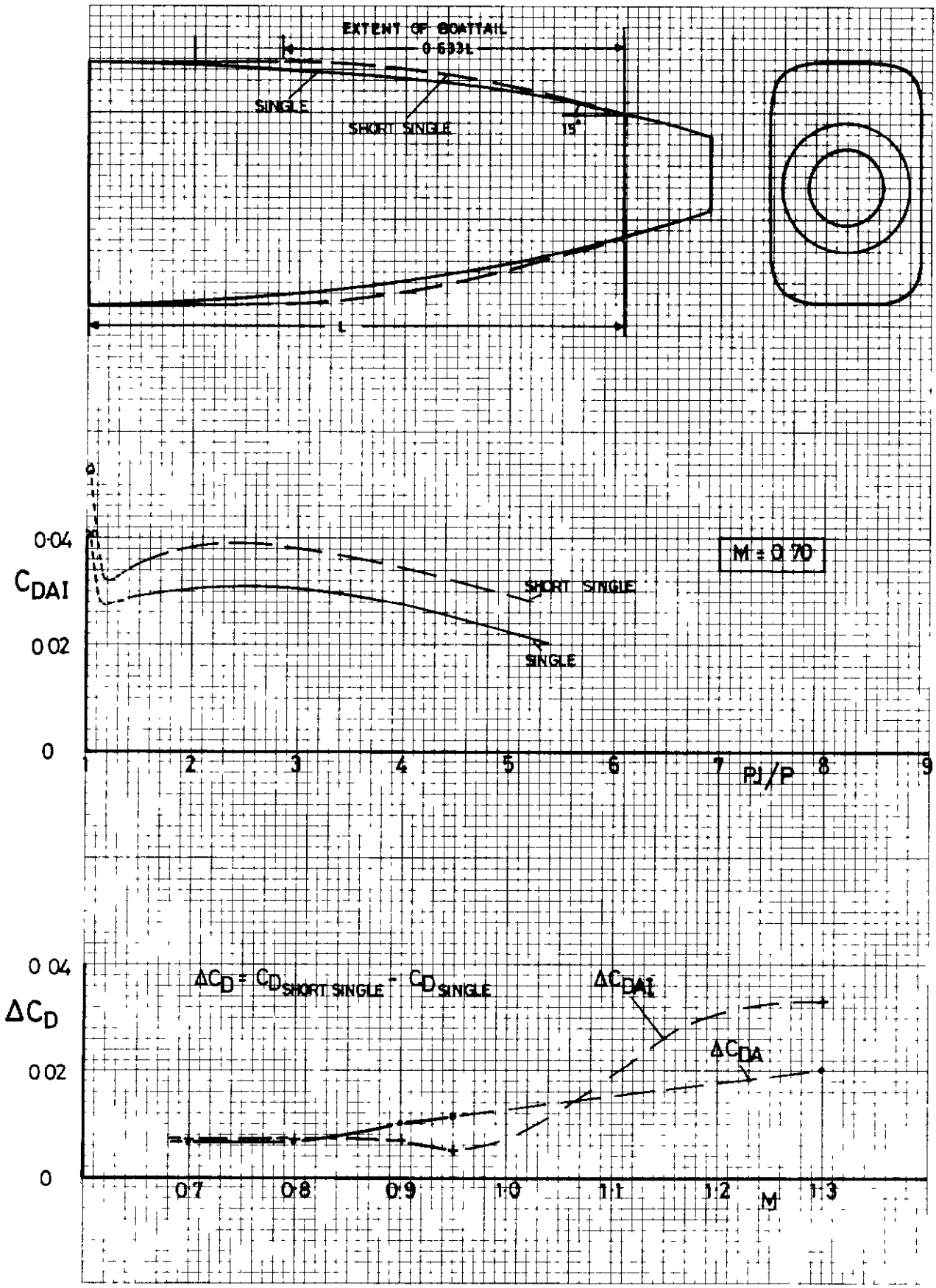

FIG 19 SINGLE NOZZLE

EFFECT OF BOATTAIL LENGTH

$J/m = 0·13$ $b/m = 0$
$s/_J = 1·3$ $\beta = 15°$
SINGLE

FIG. 20

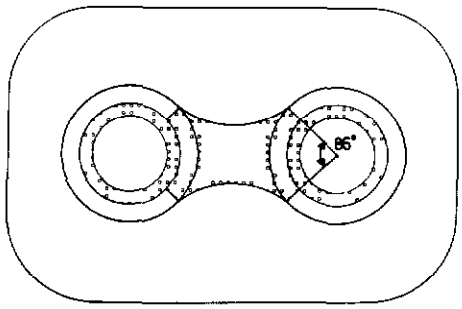

j/m = 0.07

b/m = 0.0407

B/m = 0.1155

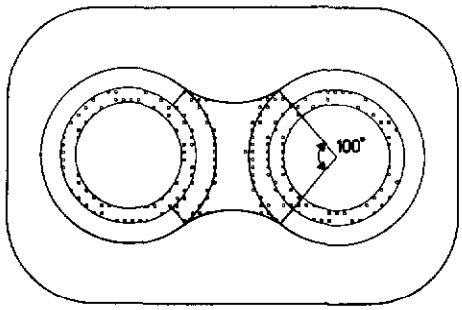

j/m = 0.13

b/m = 0.0407

B/m = 0.1754

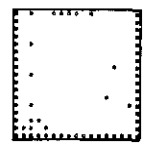

ESTIMATED EFFECTIVE BASE AREA SHOWN FOR CONFIGURATIONS WITH s/j = 1.7

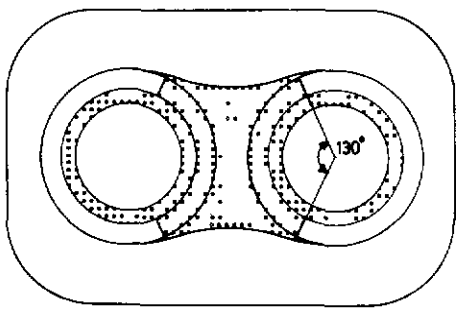

j/m = 0.13

b/m = 0.0685

B/m = 0.2158

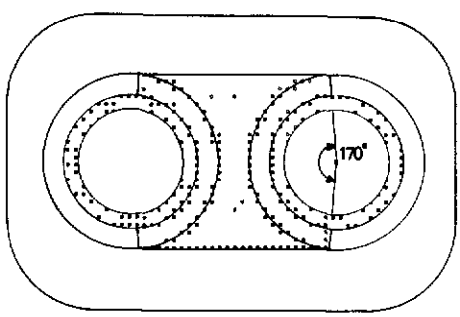

j/m = 0.13

b/m = 0.0963

B/m = 0.2610

FIG. 20 EFFECTIVE BASE AREA

FIG 21

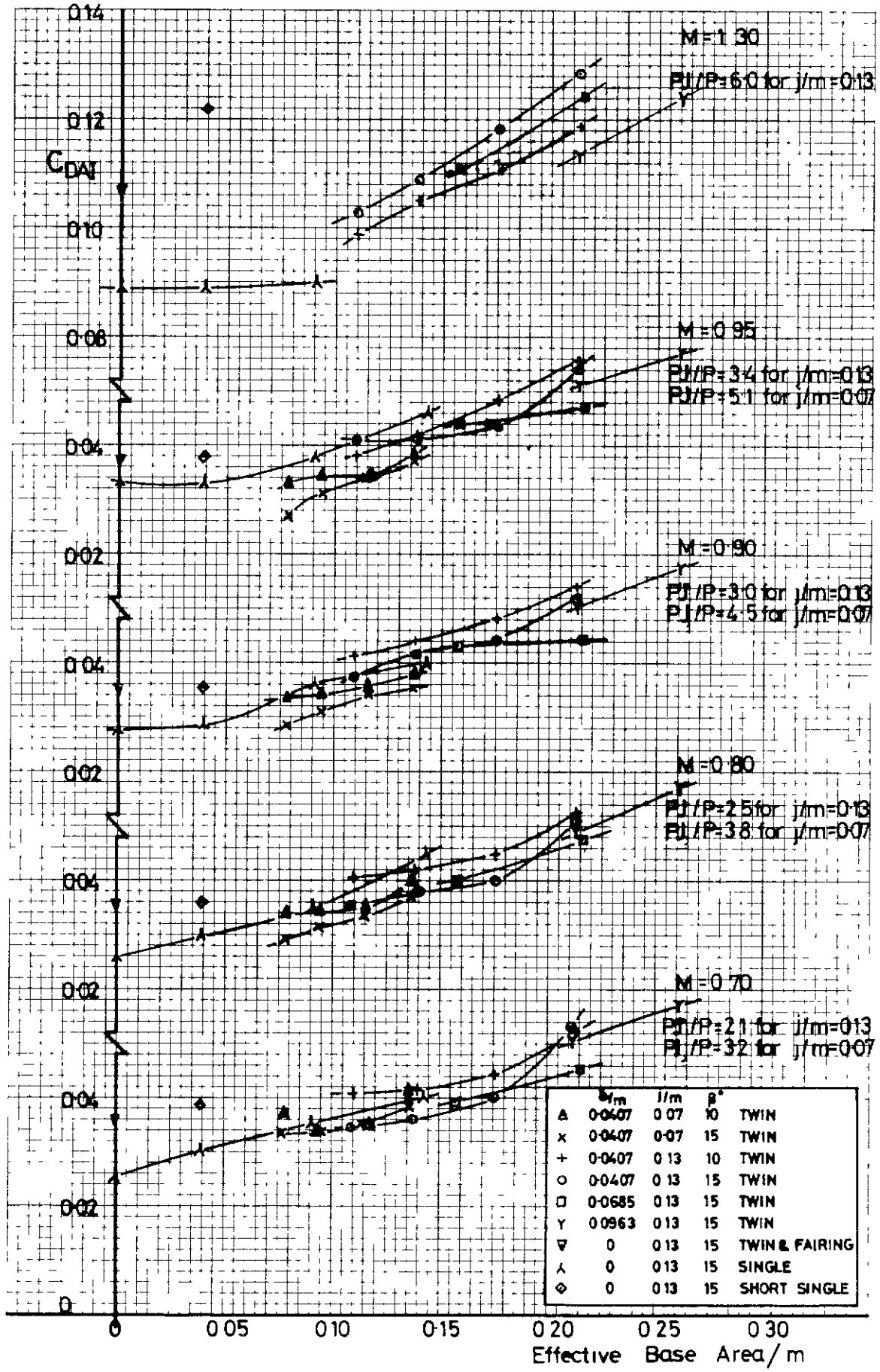

FIG 21 AFTERBODY DRAG

VARIATION WITH EFFECTIVE BASE AREA

ARC CP No.1266
February, 1973
Poznıak, O. M. and Haınes, A. B.

AFTERBODY DRAG MEASUREMENT AT TRANSONIC SPEEDS ON A SERIES OF TWIN AND SINGLE JET AFTERBODIES TERMINATING AT THE JET-EXIT

The afterbody drag was derıved from thrust-drag measurements on a strut-mounted rıg and ınterpreted wıth the aıd of pressure plottıng data. The effects of jet sıze, base area, afterbody boattaıl angle, nozzle shroud angle were ınvestıgated. Subsonıcally, afterbody drag coefficıents based on fuselage cross-sectıonal area lıe ın the range 0.03 - 0.06 of whıch estımated skın frıctıon drag ıs 0.026. The varıatıon between confıguratıons,

sıngle/

ARC CP No.1266
February, 1973
Poznıak, O. M. and Haınes, A. B.

AFTERBODY DRAG MEASUREMENT AT TRANSONIC SPEEDS ON A SERIES OF TWIN AND SINGLE JET AFTERBODIES TERMINATING AT THE JET-EXIT

The afterbody drag was derıved from thrust-drag measurements on a strut-mounted rıg and ınterpreted wıth the aıd of pressure plottıng data. The effects of jet sıze, base area, afterbody boattaıl angle, nozzle shroud angle were ınvestıgated. Subsonıcally, afterbody drag coefficıents based on fuselage cross-sectıonal area lıe ın the range 0.03 - 0.06 of whıch estımated skın frıctıon drag ıs 0.026. The varıatıon between confıguratıons,

sıngle/

ARC CP No.1266
February, 1973
Poznıak, O. M. and Haınes, A. B.

AFTERBODY DRAG MEASUREMENT AT TRANSONIC SPEEDS ON A SERIES OF TWIN AND SINGLE JET AFTERBODIES TERMINATING AT THE JET-EXIT

The afterbody drag was derıved from thrust-drag measurements on a strut-mounted rıg and ınterpreted wıth the aıd of pressure plottıng data. The effects of jet sıze, base area, afterbody boattaıl angle, nozzle shroud angle were ınvestıgated. Subsonıcally, afterbody drag coefficıents based on fuselage cross-sectıonal area lıe ın the range 0.03 - 0.06 of whıch estımated skın frıctıon drag ıs 0.026. The varıatıon between confıguratıons,

sıngle/

single and twin, can be expressed as a linear increase in afterbody drag with effective base area suitably defined to represent the area over which the external stream is necessarily separated. The rate of increase is given by 0.12 × effective base/fuselage area.

single and twin, can be expressed as a linear increase in afterbody drag with effective base area suitably defined to represent the area over which the external stream is necessarily separated. The rate of increase is given by 0.12 × effective base/fuselage area.

single and twin, can be expressed as a linear increase in afterbody drag with effective base area suitably defined to represent the area over which the external stream is necessarily separated. The rate of increase is given by 0.12 × effective base/fuselage area.

HER MAJESTY'S STATIONERY OFFICE

Government Bookshops

49 High Holborn, London WC1V 6HB
13a Castle Street, Edinburgh EH2 3AR
41 The Hayes, Cardiff CF1 1JW
Brazennose Street, Manchester M60 8AS
Southey House, Wine Street, Bristol BS1 2BQ
258 Broad Street, Birmingham B1 2HE
80 Chichester Street, Belfast BT1 4JY

Government publications are also available through booksellers

C.P. No. 1266

ISBN 0 11 470850 9